Chapter 3

TiO_2 -Based Surfaces with Special Wettability – From Nature to Biomimetic Application

Jian-Ying Huang and Yue-Kun Lai

Additional information is available at the end of the chapter

http://dx.doi.org/10.5772/60826

Abstract

Super-wetting/antiwetting surfaces with extremely high contrast of surface energy and liquid adhesion have attracted a lot of interest in both fundamental research and industry. Various types of special wetting surfaces can be constructed by adjusting the topographical structure and chemical composition. In this chapter, recent advance of the super-wetting/antiwetting surfaces with special solid/liquid adhesion has been reviewed, with a focus on the biomimetic fabrication and applications of TiO_2-based surfaces. Special super-wettability examples include lotus-leaf-inspired surfaces with low adhesion, rose-petal-inspired surfaces with high adhesion, spider silk bio-inspired surfaces with directional adhesion, fish-scale-inspired underwater superoleophobic surface, and artificial surfaces with controllable or stimuli-responsive liquid adhesion. In addition, we will review some potential applications related to artificial antiwetting surface with controllable adhesion, e.g., self-cleaning, antifogging/anti-icing, micro-droplet manipulation, fog/water collection, water/oil separation, anti-bioadhesion, micro-template for patterning, and friction reduction. Finally, the difficulty and prospects of this renascent and rapidly developing field are also briefly proposed and discussed.

Keywords: Wettability, Super-wetting/antiwetting, Adhesion, TiO_2-based surface, Application

1. Introduction

During the past decades, super-antiwetting surfaces, with a water contact angle (WCA) greater than 150 °, have attracted considerable interest due to their importance in both fundamental research and practical application [1-9]. Two types of extremely super-antiwetting cases exist in nature, which are the "sliding" super-antiwetting lotus leaves or water strider with ultralow water sliding resistance and the "sticky" super-antiwetting petal effect or gecko feet with extremely high liquid adhesion. Biomimetic studies demonstrate that the synergistic effect of topographical structures and chemical compositions plays a vital role on the special functional surfaces with various adhesions. These findings have inspired the creation of super-antiwetting functional surfaces with self-cleaning, anti-icing/antifogging, water/oil separation, micro-droplet manipulation, anti-bioadhesion, micro-template, and low-friction transportation [10-16].

Figure 1. Some natural cases in lotus leaf, mosquito eye, rose petal, spider silks, butterfly wings, gecko feet, desert beetle, and water strider and their potential applications of biomimetic super-antiwetting surfaces, such as self-cleaning, anti-icing/antifogging, micro-droplet manipulation, fog/water collection, water/oil separation, anti-bioadhesion, micro-template for patterning, and friction reduction

In the following two sections, we will give a summary of super-wetting surface and super-antiwetting surfaces with specific adhesions observed in nature, as demonstrated in Figure 1, such as lotus leaf, mosquito eye, rose petal, spider silks, butterfly wings, gecko feet, desert beetle, and water strider. The corresponding bio-inspired superhydrophobic surfaces with special wettability and solid/liquid adhesion are also reviewed and discussed (super-antiwetting surfaces with weak/strong adhesion, anisotropic adhesion, or controllable/switchable adhesion). The methods to construct or regulate the adhesion of artificial super-antiwetting surfaces can be considered from two strategies. One is to adjust the chemical component or

http://dx.doi.org/10.5772/60826

change the topographical structure respectively or simultaneously. The other is to provide external stimulations to induce chemical component or surface structure transition on responsive material surface. We will also review some significant applications related to TiO_2-based surfaces with special wettability and adhesion. Finally, we briefly draw conclusion from the problems and challenges that existed on the synthesis processes and practical applications of super-antiwetting surface with special solid/liquid adhesion.

2. Surfaces with special wetting states

In general, compared to hydrophobic surfaces, artificial super-antiwetting surfaces obviously exhibit lower solid/liquid adhesion. For example, typical super-antiwetting surface usually has a low adhesive force and a sliding angle smaller than 10 °. However, some specific super-antiwetting surfaces, under comparable contact angle, have exhibited much stronger solid/liquid adhesion. Such special adhesion is highly related to the specific contact modes at the three-phase (solid/liquid/air) contact line (TCL) and the interaction at the solid/liquid interface. Recently, Wang et al. categorized five types of wetting states on super-antiwetting surfaces according to their liquid adhesion from high to low: Wenzel state and Gecko (petal) state, intermediate state, Cassie state, and lotus state [17]. A stronger adhesive force is demonstrated on the Wenzel state substrate because liquid penetrates to come in contact with the solid surface, resulting in the obvious increase of the solid/liquid real contact area. Simultaneously, the corresponding TCL becomes continuous and stable [18]. Thus with this state, the surface exhibits relatively high adhesion, and liquid droplet does not fall off easily even on the tilted substrate with a large angle. Droplets are not stable on such surface with weak solid/liquid interaction. In contrast, for the Cassie state, a large amount of air pocket is trapped between the solid and liquid interface, the real solid/liquid contact area is lower, and the TCL is highly discontinuous [19]. However, in most cases, an intermediate state between Cassie and Wenzel states is generally found with partial air trapped in the solid/liquid interface. Such an intermediate state is not stable and preferentially changed to the Wenzel contact state under external stimuli. This means that solid/liquid adhesion on such super-antiwetting substrate can be adjusted to some extent without the change of solid surface compositions and morphologies. Therefore, controllable solid/liquid adhesions can be realized base on the manipulation of surface outmost composition, topographical structure, and external stimuli.

Normally, the solid/liquid adhesive force can be qualitatively assessed by the sliding angle (contact angle hysteresis), which is usually defined as the contrast between advancing and receding contact angles. The sliding angle on superhydrophobic surfaces can be influenced by the topography, structure, chemical heterogeneity, TCL, etc. In the following sections, various types of super-wetting/antiwetting surfaces are taken into account according to their special adhesion items. Moreover, we mainly discuss the mechanism for TiO_2-based composites with special wetting states, and the corresponding wettability or adhesion adjustment and their practical or potential applications will be presented in other sections.

2.1. Super-wetting surfaces with high surface energy

In 1997, Fujishima et al. reported the UV-induced superamphiphilic ability of a single-crystal rutile TiO_2 surface [20]. Before UV illumination, the TiO_2 surface displayed a water contact angle of 72 °. However, the droplets completely spread on the film after UV illumination for certain duration. This is due to the creation of numerous high-energy domains with hydrophilic/oleophilic property on TiO_2 surface. Moreover, the wettability of either polycrystal or single-crystal TiO_2 surfaces could be reversible between hydrophobicity and superhydrophilicity under the alternation of long-term dark storage and UV light irradiation, independent of their photocatalytic properties. After the discovery of light-induced superamphiphilic ability on TiO_2 surfaces, great attention has been paid to explicate the mechanism of such unique wetting transition under UV light [21]. In addition to the pristine single-crystal TiO_2, the polycrystalline TiO_2-based thin film also exhibited photo-induced amphiphilicity. Although another inherent photo-induced phenomenon can take place simultaneously on the identical TiO_2-based surface, the photocatalysis-induced hydrophilicity demonstrated intrinsically different processes and mechanisms to that of abovementioned photo-induced hydrophilicity. It has been believed that the combination of structure/component changes and the photocatalytic degradation of low energy hydrocarbon groups at TiO_2-based surface is the main reason for the realization of photocatalysis-induced hydrophilic ability. Utilizing these two inherent abilities of TiO_2, a wide variety of super-wetting TiO_2 materials have been prepared, exhibiting environmental friendly applications in self-cleaning, antifogging, and other fields. In this section, we will focus on the recent developments in super-wetting TiO_2-based materials by various techniques with or without the assistance of UV light activation.

Fujishima et al. reported TiO_2/SiO_2 nanostructure composited films with super-wettability under UV irradiation [22]. The top TiO_2 layer with photocatalysis and photo-induced super-wetting and the bottom porous SiO_2 layer with low refractive index provided promising outdoor uses for self-cleaning and antifogging/reflection. Shang et al. reported N- and F-codoped TiO_2 nanotube arrays with palladium oxide nanoparticles decoration [23]. These codoped TiO_2 nanotube arrays exhibited a fast visible light-induced super-wetting due to its superior photocatalytic property and special vertical alignment, which has promising applications in self-cleaning.

Electro-wetting proved to be a versatile method to significantly decrease the contact angle of partially wetting droplets on solid substrates with an externally applied voltage [24]. Recently, Ma et al. reported that an electric polarization process would enhance surface hydrophilicity of microarc-oxidized TiO_2 coatings by taking advantage of the electro-wetting effect [25]. Although the electric polarization treatment could not alter the surface roughness, this approach resulted in surface electric fields and produced surface charges. Owing to the electric polarization, the electrostatic forces decreased the surface energy and the contact angle, resulting in the durable wettability.

Recent studies also demonstrated that the thermal treatment can increase the antiwetting ability of TiO_2 films. Meng et al. fabricated TiO_2 layers with thermo-induced hydrophilicity on silicon or quartz substrates by radio-frequency magnetron sputtering [26]. It was found that the crystal structure played a vital role in the surface wettability of TiO_2 layers. When the

http://dx.doi.org/10.5772/60826

annealing temperature was about 900 °C, the mixture of anatase and rutile induced optimal hydrophilicity.

UV or visible light illumination is an effective approach for the creation of super-wetting TiO_2-based surfaces. However, it is promising to construct TiO_2 layers possessing persistent super-wetting without the need of external stimuli. Utilizing a facile electrophoretic process for the deposition of charged nanotube particles prepared by hydrothermal approach (Figure 2a, b), a super-wetting cross-stacked TiO_2-based thin films with good mechanical adhesion were successfully coated on a conductive glass substrate (Figure 2c, d) [27]. Without the use of UV illumination, the TiO_2 layers displayed superhydrophilic property with a rapid droplet spreading within 0.16 s (Figure 2e). This can be ascribed to the porosity effect and surface hydroxyl, which played an important role in controlling the interaction between the liquid and film.

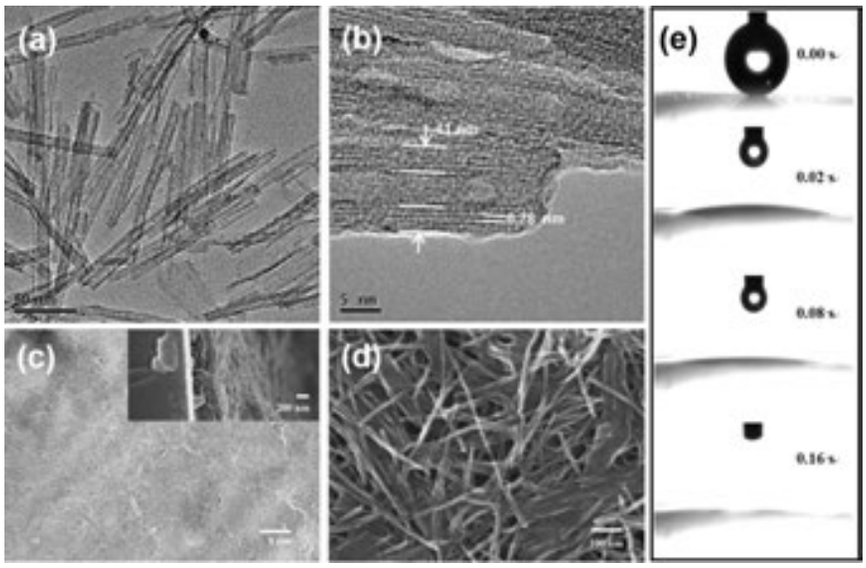

Figure 2. (a, b) TEM images of titanate nanotube prepared by hydrothermal approach; (c, d) the SEM images of titanate nanotube film by a facile electrophoretic deposition (EPD) process; and (e) the liquid wetting behavior on porous superhydrophilic TiO_2(B) surface. The inset figure is the corresponding cross-sectional image of deposition film

Fu et al. fabricated superhydrophilic surfaces with the micro-nano dual-scale hierarchical structures using SDBS-modified TiO_2 nanoparticles [28]. These films exhibited superhydrophilicity without the requirement of UV irradiation, arising from the high surface roughness. This work opened an avenue to construct functional TiO_2 for promising applications in self-cleaning and antifogging without UV irradiation. Funakoshi et al. fabricated superhydrophilic TiO_2 thin films on glass substrate surfaces through the titanium alkoxide hydrolysis [29]. Zeng et al. prepared transparent nanosized crack-free TiO_2 thin films with good adhesion to glass substrates through a self-assembly approach. This method consisted of the preparation of TiO_2 colloidal particles and adsorptive self-assembly in the colloidal stock and followed by heat treatment [30]. The resultant films exhibited superhydrophilicity with a water contact angle of about 0 ° and still retained at about 15 ° even after the dark storage for a week.

Moreover, these self-assembled TiO_2 films presented high transmittance and excellent photocatalytic activity.

2.2. Super-antiwetting surfaces with low adhesion

In nature, many biological creatures possess the combination of low-energy surfaces and hierarchical structures that endow the super-antiwetting properties with weak adhesion. Among them, the water stride and lotus leaf are two of the most classic examples [31, 32]. The phenomenon of collecting the dirty debris by the sliding of water droplets on lotus leaf surface is commonly known as the "lotus effect." The lotus leaf therefore always keeps itself clean by this self-cleaning behavior. Bio-inspired by the self-cleaning effect of lotus leaves, different artificial superhydrophobic TiO_2-based surfaces with low adhesion have been created by the construction of surface-roughened structures with suitable chemical compositions [33-40].

Bhushan et al. created different self-cleaning superhydrophobic structures by the replication of a micropatterned silicon substrate using an epoxy resin and hydrophobic alkane coating [41]. They investigated the effect of lotus-like structures on wetting and self-cleaning efficiency. The main factor of hierarchical structure for superhydrophobicity with low adhesion was also revealed. Zhou et al. fabricated superhydrophobic metallic oxide layer on titanium or aluminum substrates with a combination of electrochemical anodizing and self-assembly technique [42]. In comparison with the smooth surface, the porous metallic oxide exhibited excellent self-cleaning ability and can be stabilized over a wide range of pH value. Jiang's group successfully constructed artificial water strider leg with a ribbed conical nano-needle structure containing oriented nano-grooves sculptured on the lateral nano-needle surface [43]. Such artificial leg exhibited good dynamic stability under loading and during load relaxation. In addition to the implication for the design of stable superhydrophobic structure surfaces, this work provided inspiration for the applications in drag-reduction fields and miniaturized aquatic devices.

While many techniques have been developed to fabricate superhydrophobic surfaces by creating roughened surfaces and/or changing the surface energy, these techniques are limited by the types of materials to be treated. The direct coating of highly hydrophobic powder by spinning or spraying on various substrates was verified to be a facile method to construct surface with superhydrophobic property. For example, to demonstrate the versatility of the current approach, we have prepared the superhydrophobic on a silicon substrate, lab rubber glove, and A4-size printing paper by spraying, spin coating, or dip coating [44]. It is also interesting to note that the cross-stacked microscale/nanoscale fluorinated titanium nanobelt structures are formed on substrate (Figure 3a, b). Water droplet is easy to roll off due to the ultralow solid/liquid adhesion and bounce off the decorated silicon surface when it is dropped from a certain height (Figure 3c).

2.3. Super-antiwetting surfaces with high adhesion

In contrast to conventionally super-antiwetting surfaces (lotus leaves and water stride's legs) with low adhesion, there are some other biological surfaces (rose petals and gecko toes) on which water droplets are firmly pinned meanwhile kept with a contact angle larger than 150 °

http://dx.doi.org/10.5772/60826

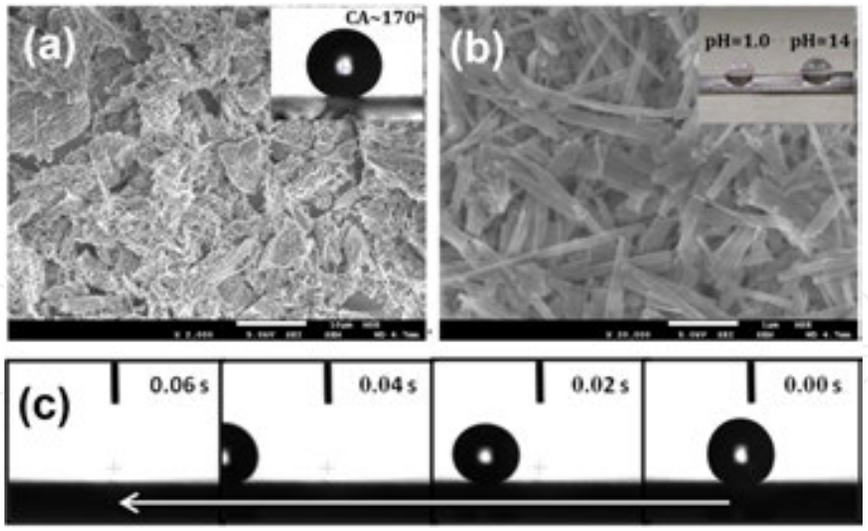

Figure 3. SEM image of cross-stacked microscale/nanoscale fluorinated titanium nanobelt particles formed on silicon substrate and the corresponding water droplet behavior on particle-decorated surface

[45-47]. To discover the mechanism of such special high adhesion, Feng et al. investigated the microstructures of rose petal and found that topographical surfaces of rose petal are made up with a periodic array of micro-papillae with compactly arranged structures and numerous nanoscale cuticular folds on micro-papillae [47]. Water droplets are expected to penetrate into the microscale papillae, but a large amount of air trapped inside the nanoscale folds resulted in the formation of specific petal-like wetting state with high adhesion. Inspired by the adhesion mechanism of rose petals and geckos, several efforts have been paid to prepare sticky super-antiwetting surfaces, on which a droplet does not slide even with a tilting angle of 90 degrees [48-53]. For example, Jiang et al. successfully fabricated well-aligned super-antiwetting polystyrene nanotube array films with high hysteresis by using anodized alumina membrane templates [48]. They believed that the main reason responsible for the great adhesion is the enhancement of van der Waals forces between the densely packed nonpolar polystyrene nanotubes in close contact with droplet. Guo et al. reported a facile method to construct sticky superhydrophobic surface via etching of an aluminum alloy surface and eliminating its loose layer [49]. They subsequently demonstrated that a much stronger adhesion by the joint action of capillary forces and van der Waals forces from the micro-orifices and hydrophilic nanoparticle composite structures.

Recently, Lai et al. reported a facile electrochemical anodizing process to construct TiO_2 nanopore structure surface on Ti substrate (Figure 4a, b) [54]. Compared to the hydrophobic of smooth Ti surface, the nanopore structure surface exhibited a superhydrophobic property (Figure 4c, d). Moreover, such specific superhydrophobic structure displayed a very strong adhesive force of 75.6 μN (Figure 4e), which resulted from the van der Waals attraction between the water molecules and fluoroalkylsilane molecules and from the negative pressure caused by the volume change of air sealed in the nanopore units. As a result, the bead was firmly pinned on such sticky superhydrophobic surface without any movement when it was tilted to a vertical position (Figure 4f) or even when turned upside down.

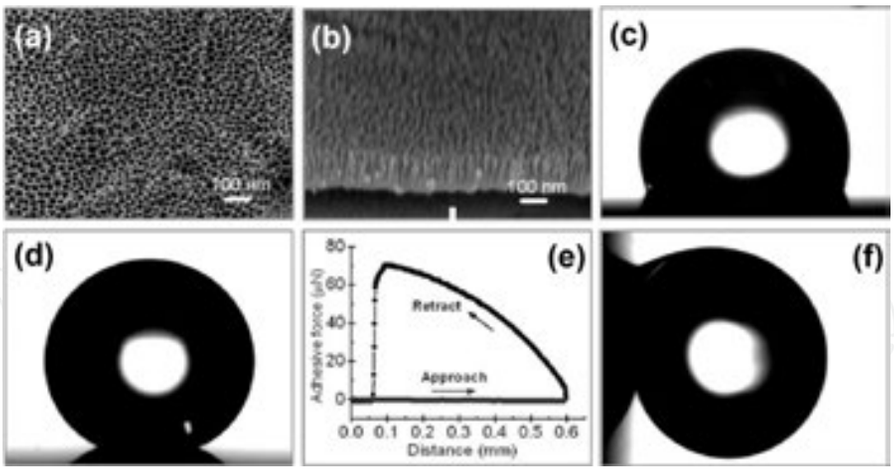

Figure 4. (a, b) Top-view and side-view SEM images of TiO_2 nanopore structure. (c) Photo of a water droplet on the TiO_2 flat surface with PTES modification. (d) Droplet on the superhydrophobic TiO_2 nanopore film. (e) The force-distance curves recorded before and after the superhydrophobic surface made contact with a droplet. (f) A water droplet on a highly adhesive superhydrophobic surface vertically tilted

2.4. Super-antiwetting surfaces with controllable adhesion

2.4.1. Effect of morphology and structure

Based on the theoretical background of wetting, it is easy to understand that the great effect of morphological and structural parameters on the determination of wetting models and contact TCL situation and resultant to influence the droplet adhesion on super-antiwetting surfaces. For the identical material with certain surface energy, the solid/liquid adhesive force can be controlled by tailoring the morphology or the scale of the structures on the surface [55-59]. Accordingly, we designed and constructed three kinds of unique super-antiwetting TiO_2 nanostructure models, e.g., a nanotube array (NTA), a nanopore array (NPA), and a nanovesuvianite structure (NVS) by a facile electrochemical anodizing process (Figure 5) [54]. These different structures with various wetting states and controllable porosities could effectively change the air-pocket ratio in sealed and open systems, so that the solid/liquid adhesive force could be achieved in a wide range. Capillary adhesive force plays a dominant role in imparting adhesive behavior on NTA and NPA nanostructures due to the formation of sealed air pockets, while the NVS nanostructures exhibit extremely low adhesion due to the absence of sealed air pockets. In addition, adhesive forces could be tuned by changing the nanotube diameter, especially the tube length, due to the negative pressure caused by the volume change of air sealed in the nanotubes. The cooperation effect between the negative pressures induced by the volume change of sealed air pockets and the van der Waals attraction at solid/liquid interface contributes to the water adhesion. These findings are valuable to deepen insight into the roles of nanostructures in tailoring water repellency and adhesion for exploring new applications. Lee et al. further verified that the liquid adhesion could be controlled by tuning the formation ratio of dead-end nanopores on superhydrophobic anodized aluminum oxide [60, 61].

http://dx.doi.org/10.5772/60826

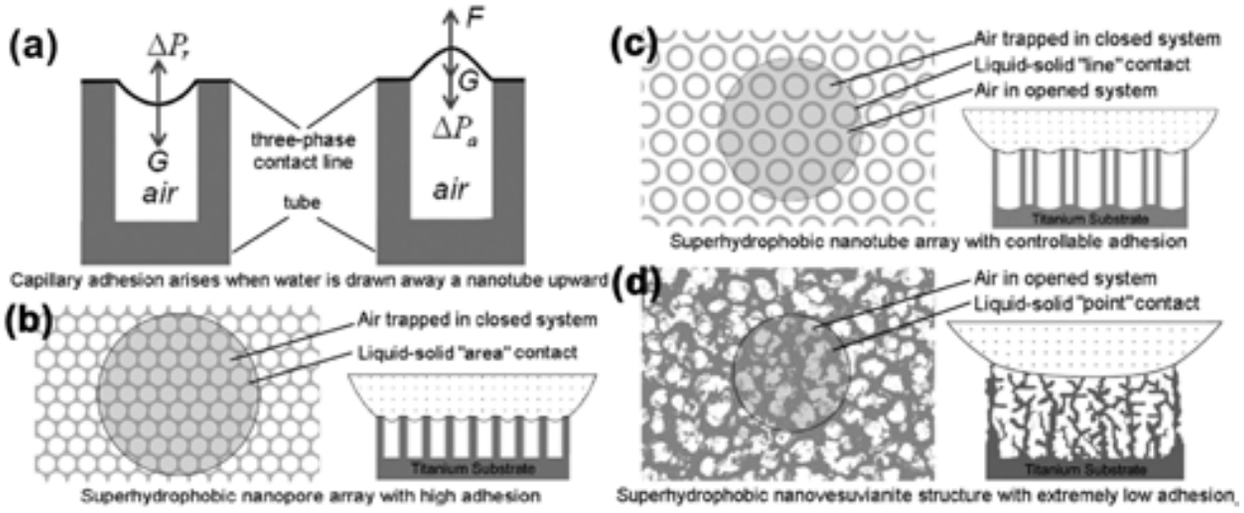

Figure 5. Schematic illustration of three types of super-antiwetting nanostructure models with different adhesions. (a) Schematic illustration of capillary adhesive force caused by negative pressure when a water droplet is drawn away an NPA or NTA close system; (b) super-antiwetting NPA with high adhesion; (c) super-antiwetting NTA with controllable adhesion; and (d) super-antiwetting NVS with extremely low adhesion

2.4.2. Effect of chemical composition

The chemical component with certain surface energy is another key factor in determining the wettability and solid/liquid adhesion. For a super-antiwetting surface with identical morphology, the solid/liquid adhesive force could be greatly controlled by utilizing the difference in the alkyl chain length or by adjusting the ratio of high-energy hydrophilic areas [62-66]. Recently, we reported a successful case of the super-antiwetting spongy-like TiO_2 film exhibiting adhesion ranging from 5.0 μN (ultralow) to 76.6 μN (extremely high) by adjusting the dosage concentration of high-surface-energy materials of nitrocellulose (Figure 6) [62]. The super-antiwetting films without the introduction of NC displayed an exceptionally low adhesion with a sliding angle of only approximately 0.8°. However, the nitrocellulose modified super-antiwetting film can firmly catch liquid droplets even when it is turned upside down, indicating high adhesion to droplets. Such significant adhesion enhancement was ascribed to the fact that the introduction of hydrophilic nitro groups not only leads to the formation of hydrogen bonding with the hydroxyl groups at the solid/liquid interfaces but also result in the disruption of the dense alignment of hydrophobic silane molecule.

Other techniques for constructing sticky super-antiwetting layer are based on terminating of high-surface-energy groups on rough structures or site-selective discomposing of low-surface-energy chains to obtain patterned surface with micrometer-scale chemically heterogeneous composition [67-69]. For example, Wang et al. realized switchable wettability and reversible adhesion between sticky superoleophobicity and sliding superoleophobicity by alternating annealing treatment and UV illumination on TiO_2 nanostructure surfaces [67]. However, most of the abovementioned techniques cannot rapidly and in situ change the wettability and adhesion.

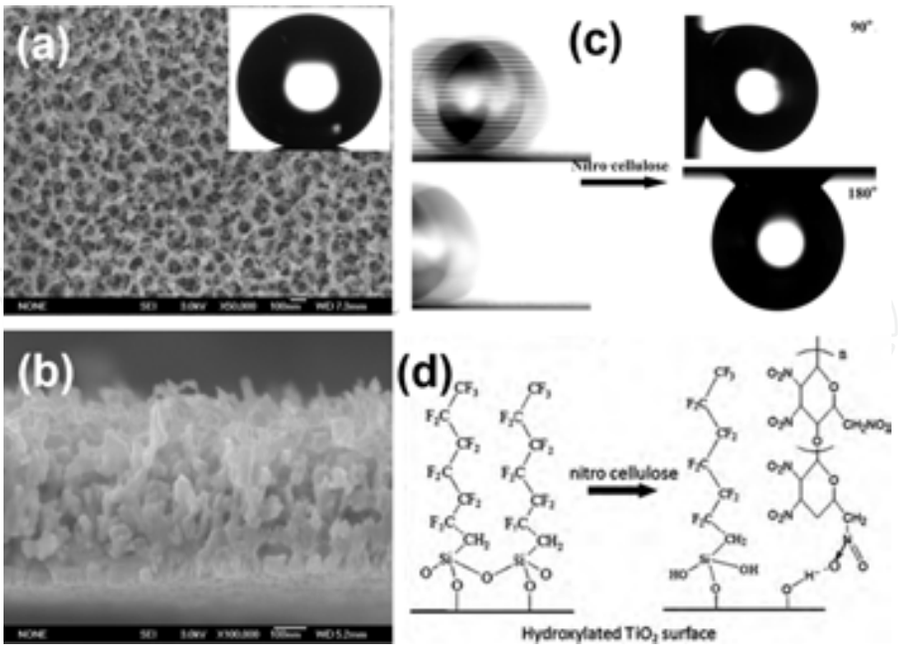

Figure 6. Top-view (a) and side-view (b) SEM image of a sponge-like TiO_2 nanostructure film on Ti substrate. The inset of (a) shows the droplet image on corresponding superhydrophobic TiO_2 surface. (c) Behavior of a water droplet on sponge-like TiO_2 surface before and after NC introduction. (d) Model of molecular self-assembly before and after NC introduction

In contrast to the top-down photo-cleavage of chemical components to control the liquid adhesion on superhydrophobic surface, herein, we realized that both water wettability and adhesion change with a large degree of contrast on superhydrophobic TiO_2 nanotube array film via a facile, in situ bottom-up ink combination to simultaneously regulate topographical structure or chemical components at targeted places (Figure 7) [70]. The site-specific ink covering and removal allows the wettability and reversible adhesion transitions to be realized. These techniques are helpful to effectively construct novel functional nanomaterials with customer-tailored surface wettability and adhesion [71].

2.5. Super-antiwetting surfaces with responsive adhesion

Recently, intelligent surfaces with responsive wettability and adhesion that can reversibly change between highly hydrophilic (strong adhesion) and hydrophobic (weak adhesion) have attracted much attention due to their practical applications. As we have known, the wetting state has a strong influence of droplet adhesion on super-antiwetting surface. The change of contact angle hysteresis (decreasing of the receding angle) is a key factor to control droplet mobility on surfaces. In general, Wenzel-state super-antiwetting surfaces exhibit higher droplet adhesion, while the adhesion will be dramatically decreased on Cassie wetting-state surfaces. There exist certain energy barriers to prevent the spontaneous transition between these two wetting states. If a molecule can reversibly alter its surface energy on a hierarchical surface to induce the change of contact model, such smart surface whose wettability can be modulated between highly hydrophilic and hydrophobic, or even super-wetting and super-antiwetting, can be realized (Figure 8a). In contrast, if a specific molecule can alter its polarity

http://dx.doi.org/10.5772/60826

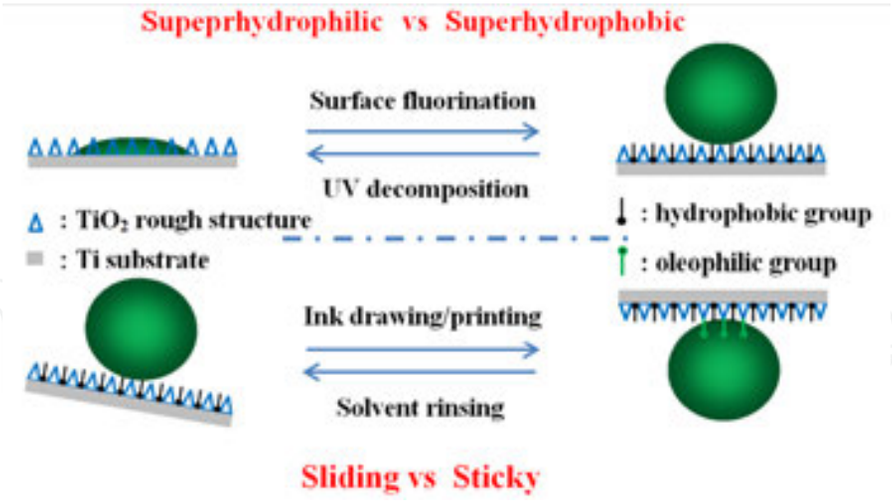

Figure 7. Schematic representation of the mechanism of wettability and adhesion on robust superhydrophobic TiO_2 rough structure prepared via a facile electrochemical anodizing strategy for TiO_2 nanotube construction, surface fluorination, and reversible site-specific ink printing/removing

but without greatly changing the surface energy of a hierarchical structured surface, a super-antiwetting surface with controllable adhesion can be achieved. The mobility of droplet behavior on such surfaces can be controllably switched from sticky to a sliding state (Figure 8b). Based on this strategy, various types of smart-responsive materials, such as polymers, liquid crystal molecules, and semiconducting inorganic oxides can be utilized to achieve wettability switches that are controlled by external stimuli. Therefore, if an external stimulus can be applied to induce the transition, the wettability and droplet adhesion will be reversibly switched.

Recently, stimuli-responsive surface wettability has been extensively studied under external stimulus such as light irradiation [72-74], electric field [75-79], thermal treatment [80, 81], magnetic field [82, 83], transformation [84, 85], pH [86], and multi-responsive factors [87, 88]. Among them, light irradiation and photoelectric cooperative wetting can be facilely used to achieve liquid patterns for printing, which is also promising to gear up the scientific investigation in the fields of biological and health sciences and broadened their practical applications. Inorganic TiO_2 semiconductor is an important photo-responsive multifunctional material. For example, responsive water-droplet adhesion between sliding and pinned states on a superhydrophobic polythiophene film constructed by a versatile electrodeposition method is realized by adjusting electric potential [89]. In recent years, smart wettability-responsive surfaces with reversibly switching between superhydrophilicity and superhydrophobicity have attracted increasing interests. Recently, Zhou et al. demonstrated a facile method to achieve reversible change of adhesion to water droplets without loss of superhydrophobicity [90]. The super-antiwetting TiO_2 surface was illuminated with UV through a mask to create alternatively arranged hydrophilic/superhydrophobic domains. Photo-induced hydrophilic regions increased water adhesion, and surrounding super-antiwetting regions prevented the spread of water droplets and preserved super-antiwetting. The recovery was very fast upon heating at a relatively high temperature or the use of microwaves. The TiO_2 nanotube array

surface presented a UV-thermal-induced reversible adhesion switching attributed to the displacement of C-F groups and introduced -OH groups upon site-specific UV irradiation, which can increase droplet interaction with superhydrophobic surface. The heat treatment resulted in the decrease of high-energy Ti-O-H bonds and the restoration of hydrophobic C-F bonds with low surface energy, showing the primary Cassie superhydrophobic state.

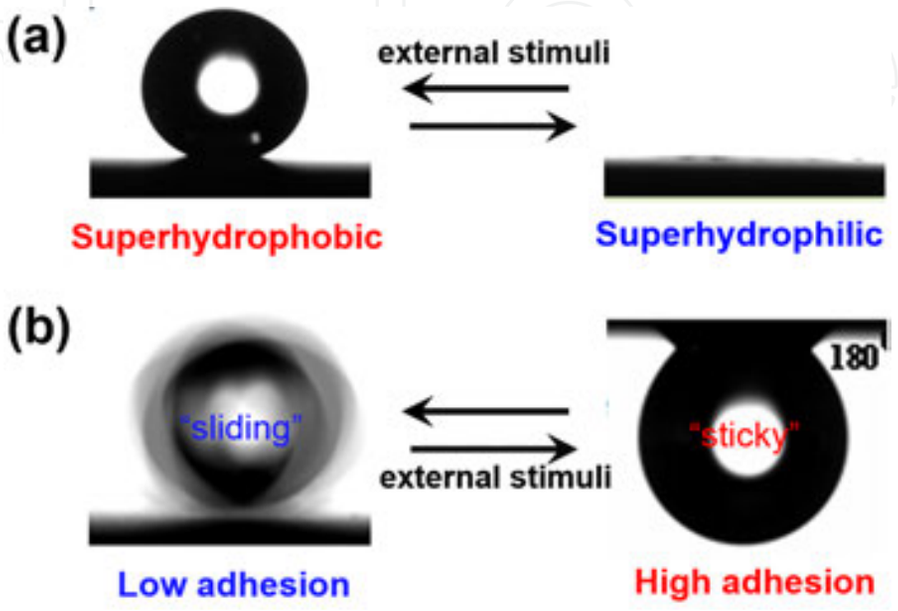

Figure 8. (a) Reversible switching wettability on smart surfaces between superhydrophobicity (left) and superhydrophilicity (right) by external stimuli. (b) Reversible switching of solid/liquid adhesion with extremely high contrast on a superhydrophobic smart surface

2.6. Super-antiwetting surfaces with anisotropic adhesion

If a surface displays different contact angles or sliding angles under various directions, such surface is stated to be anisotropic in wettability. Directional droplet manipulation as a vital process for biological system is ubiquitous in nature. For example, anisotropic super-antiwetting surfaces allow spider silk to collect water, butterflies to shed off droplets, and plants to trap insects and pollen. Butterfly wings have directional adhesion [91]. Droplets can easily roll off the wings along the radial outward direction of the central axis of the butterfly body while it is firmly pinned in the opposite direction. Recent investigations verified that anisotropic wettability and adhesion were highly related to the anisotropic three-phase contact line [92, 93]. Recently, anisotropic wetting surfaces have attracted a great amount of attention in various fields due to their specific advantage, such as microfluidic devices, and self-assembled pattern synthesis.

Micropatterned wettability surfaces displaying anisotropic sliding and adhesion in a high contrast to droplets have the ability to directionally manipulate micro-droplets and many promising applications in lab-on-a-chip and high-throughput fluidic devices [94]. By taking advantage of adhesion anisotropy, the on-demand manipulation of droplets is feasible. Figure

http://dx.doi.org/10.5772/60826

9 displays the effects of ink unit (dot or line) size and liquid volume on mobility of micro-droplet on a superamphiphobic film. In general, the sliding angle increased upon decreasing the volume of the droplet, regardless of tilting direction and pattern shape (Figure 9a). For dot patterning surface, the mean value of sliding angle along various directions is found very closely, indicating similar isotropic wetting property. However, the line patterning surface additionally exhibited a directionally dependent droplet shape and sliding angle (Figure 9b). On the tilted substrate, small droplets located on the thicker line against the orthogonal direction are stable than that on the thinner line along with the parallel direction. Such strong anisotropy of sliding angle and droplet distortion on line patterning surfaces was ascribed to the high contrast of energy barrier, solid/liquid/air phase contact line, and wetting behavior along an orthogonal or parallel direction.

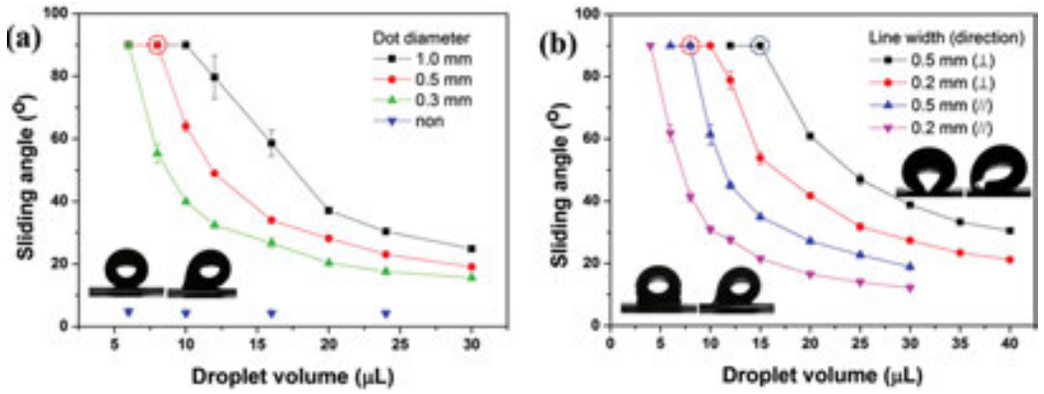

Figure 9. Droplet sliding angles on a) dot and b) line patterned superamphiphobic surface with respect to patterning size, droplet volume, and tilting direction. Insets in (a) are side-view optical images of an 8 μL droplet on a 0.5 mm ink dot before (left) or after (right) tilting with an angle of 90 °. Left insets of b) are the side-view images of an 8 μL droplet on a line with 0.5 mm in width before or after a tilting angle of 90 ° from an orthogonal direction. Right insets of b) are the side-view images of a 15 μL droplet on a line with 0.5 mm in width before or after a tilting angle of 90 ° from parallel direction (right)

3. Applications of surfaces with special wettability

Wettability is a main property of surface governed not only by geometrical structure but also by chemical composition. Recently, super-wetting and antiwetting-derived material interfaces, such as superhydrophilicity, patterned superhydrophobicity, or superhydrophobicity with special adhesion (ultralow/ultrahigh adhesion or anisotropic adhesion), have attracted much attention. Superhydrophilicity and superhydrophobicity are defined based on the conventional liquid contact angle measurement. A superhydrophilic surface generally displays a water contact angle lower than 5 °. The opposite superhydrophobic case refers to surface with contact angle greater than 150 °. Such two extreme cases and their corresponding wettability patterning surfaces have attracted great interest due to their importance in both theoretical research and practical applications.

TiO_2-based nanostructures as one of the hottest semiconductor nanomaterials have been applied in many fields including environmental/energy research and biomedical implants, owing to their unique merits, e.g., good chemical and mechanical stability, as well as excellent biocompatibility, anticorrosion, and photocatalytic properties. In this section, recent progress of the bio-inspired surfaces with special wettability has been discussed, with a focus on the emerging potential applications of TiO_2-based layers. Examples include lotus-leaf-inspired low adhesion, rose-petal-inspired high adhesion, spider silk bio-inspired super-antiwetting layers with directional liquid adhesion, and biomimetic super-antiwetting layers with adjustable and smart stimuli-responsive liquid adhesion.

While the artificial super-antiwetting surfaces with special adhesion have been introduced and constructed by many research groups as discussed above, attention has also been shifted to the potential or practical applications of multifunctional surface with special wettability and adhesion in the recent few years. Some important applications, such as self-cleaning [95-100], antifogging/icing [101-110], micro-droplet transportation [111-115], water/fog collection [116-122], oil/water separation [123-129], anti-bioadhesion [130-139], micro-template for patterning [140-149], and friction reduction [150-159], could be realized through the improved understanding of super-antiwetting with various degrees of adhesion. Selected examples are discussed below. Finally, the challenges and prospects of this renascent and rapidly developing field are also briefly addressed and discussed.

3.1. Super-wetting surfaces for self-cleaning and antifogging

Since the report of TiO_2 with super-wetting under UV light illumination in 1997, a great number of applications have been focused on this multifunctional material. Water droplets can uniformly spread or be absorbed quickly into superhydrophilic substrates. As discussed in the above section, super-wetting TiO_2 surfaces can be easily constructed through UV illumination, even displaying superamphiphilic for both water and oil. Utilizing this strategy, various super-wetting TiO_2-based nanostructure materials have been fabricated, exhibiting environmental-friendly applications such as self-cleaning, antifogging, underwater superoleophobicity, and other items.

Zhai et al. recently demonstrated a multifunctional porous TiO_2 nanotube membrane with superhydrophilic-induced underwater superoleophobicity for oil-water separation, flow-through photocatalysis, and self-cleaning by taking advantage of its excellent photocatalytic oxidation activity for the degradation of pollutant or contaminated organic molecules [160]. Lai et al. prepared super-wetting cross-stacked TiO_2-based thin films with good mechanical adhesion on a conductive glass substrate [161]. Without the use of UV irradiation, the porous TiO_2 films showed superhydrophilicity with an ultrafast droplet spreading (Figure 10a). This can be ascribed to the porosity effect and high-energy-surface hydroxyl groups, which played an important role in controlling the interaction between the liquid and film. As shown in Figure 10b, the untreated quartz slide (upper) fogged immediately, and the words below are blurred by strong light scattering. In contrast, the treated slide with the coating of TiO_2(B) films (bottom) can significantly prevent fogging formation by almost instantaneously spreading and penetrating the condensed water droplets to form a thin water membrane (Figure 10c, d).

http://dx.doi.org/10.5772/60826

Therefore, the slide with the TiO_2(B)-coated glass remains highly transparent, and the words below are clearly seen.

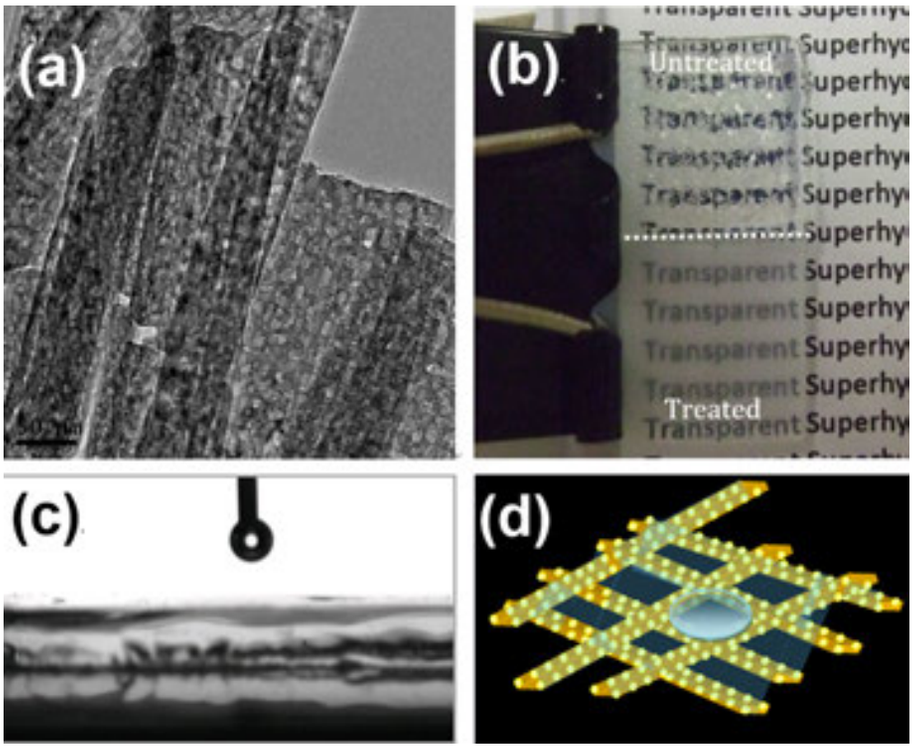

Figure 10. (a) The TEM image of porous superhydrophilic TiO_2(B) surface after calcination; (b) the liquid wetting behavior on porous superhydrophilic TiO_2(B) surface; and (c) photograph of an ITO substrate deposited with superhydrophilic coatings (bottom) and a control ITO substrate without any coating deposition (upper) taken from a refrigerator (-4 °C) to the humid laboratory air (ca. 50 % RH). (d) Schematic illustration of the ultrafast water spreading on the microscale/nanoscale pore-like superhydrophilic TiO_2(B) film. The 3D cross-aligned TiO_2(B) network and microscale and nanoscale pores result in great capillary effect to quick water invasion

3.2. Applications of Super-antiwetting surfaces

3.2.1. Self-cleaning

In nature, there exist many kinds of self-cleaning surfaces from the land to sea after hundreds of millions of years of the evolution process. As we all have known, wettability is highly related to functional surfaces with self-cleaning ability, which suggests many important hints for antifouling. Artificial technologies for self-cleaning have developed since the late twentieth century, and some achievements have led to practical applications. The applications of self-cleaning technology are very broad and vary from window glasses to solar cell panels. Three types of surfaces, including superhydrophobic, superoleophobic, and even superhydrophilic, offer solution to keep surface cleaning. Surface self-cleaning is a significant application of super-antiwetting surface. In the case of super-antiwetting rough surfaces, the solid/water interface is minimized. Water forms a spherical droplet and easily rolls off, and the droplet collects the particles from the surface. Therefore, the super-antiwetting surfaces with low

adhesion always exhibit a very low degree of contamination, which is known as self-cleaning [162, 163]. For a normal hydrophobic surface, because of the nonslip boundary condition, the water drop falls across the dirt particles and the dirt particles are mainly displaced to the sides of the droplet and redeposited behind the droplet. Ding et al. reported a long-term superhydrophobic self-cleaning coating prepared by simply blending ambient-cured fluorinated polysiloxane binder with TiO_2 nanoparticles. The obtained coating exhibited excellent wetting stability in various environments and photocatalytic self-cleaning property for practical applications [164]. Yamashita et al. fabricated super-antiwetting surfaces with photocatalytic self-cleaning abilities through coating a nanocomposite TiO_2 photocatalyst and hydrophobic layer onto a structure substrate with a co-deposition strategy [165]. This coating realizes adequate photocatalytic activity for self-cleaning and inducing unique wettability changes. The nanocomposite can contain multiple functions of energy-saving and maintenance-free characteristics. On the super-wetting surface, the water droplets spread rapidly and go beneath the contaminants to bring them away.

In addition to super-antiwetting and super-wetting, super-antiwetting of oil is also a promising characteristic for self-cleaning surfaces, which can be easily achieved in hydrophilic surfaces in water or constructed with the combination of suitable structure and chemical components. Moreover, low drag, slippery surfaces, anti-fouling, and photocatalytic activities play an important role in the self-cleaning effect. It is necessary to further develop the characterization techniques for self-cleaning surfaces. Besides pure TiO_2, some materials derived from TiO_2, such as titanate particles by hydrothermal treatment of TiO_2 particles, came into use generally for more wide applications. For example, a stable titanate nanobelt (TNB) particle suspension was prepared by a hydrogen-bond-driven assembly of pre-hydrolyzed fluoroalkylsilane (FAS) on its surface. Using this kind of TNB/FAS nanobelt, a one-step electrophoretic deposition process was applied to fabricate a cross-aligned superhydrophobic film with high transparency (up to 80 %) on glass substrate, as shown in Figure 11. Furthermore, the as-prepared coating displayed good self-cleaning ability and high chemical stability in a wide range of pH solutions [161].

3.2.2. Antifogging, anti-icing, and anticorrosion

Super-antiwetting compound eyes of mosquitoes are comprised of the smart design of elaborate microstructures and nanostructures: nanoscale of hexagonally non-close-packed nipples and microscale of hexagonally close-packed ommatidia. Such composite structures can prevent fog drops from condensing and being trapped on the super-antiwetting surface to provide an effective protective mechanism for maintaining clear vision under humid condition. Gao et al. successfully fabricated artificial super-antiwetting compound eyes by employing soft lithography methods to transfer polydimethylsiloxane micro-hemispheres and silica nano-spheres [166]. The easy rolling of water or fog droplets may take the dust particles away from the super-antiwetting compound eye-like surface with a low adhesive force, thereby achieving self-cleaning and antifogging under humid environment.

Besides the good antifogging performance, super-antiwetting surfaces can also retard the formation of frost and ice due to the metastable state of the three-phase line, compared with

http://dx.doi.org/10.5772/60826

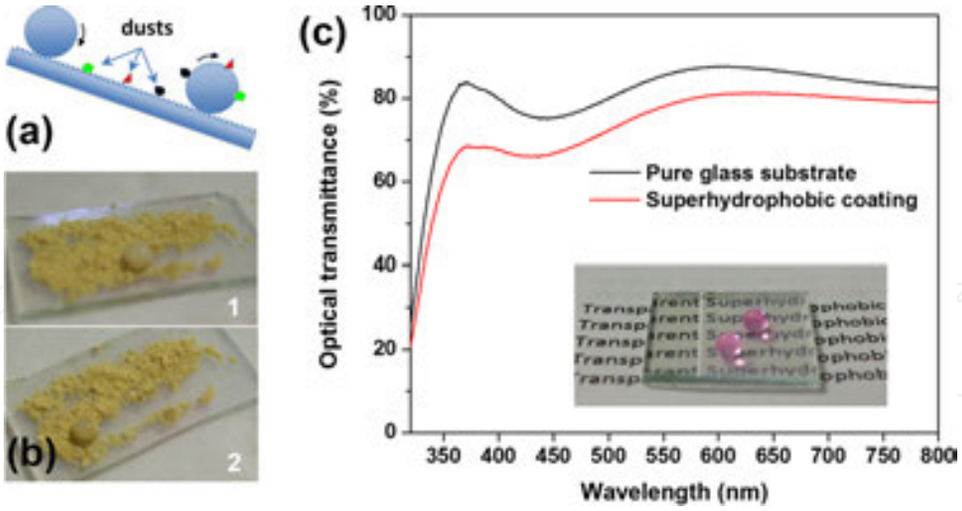

Figure 11. (a) Schematic illustration of robust superhydrophobic surface for self-cleaning. (b) Time sequence of the self-cleaning process on the superhydrophobic coating with low water adhesion. (c) Transmittance of glass substrate with or without TNB/silane hybrid films. The inset photograph of the transparent electrodeposited films with highly superhydrophobicity.

that on a smooth hydrophobic surface [104-108]. Very recently, He et al. reported the uniform ZnO nanorod array surfaces kept superhydrophobic not only to sessile macro-droplets at room temperature but also to condensed micro-droplets at temperatures below the freezing point of 5 °C or -10 °C [108]. The time of condensed droplets maintaining the liquid state (retardation period) increases with the increasing of contact angle on the superhydrophobic ZnO surfaces, indicating an obvious retardation and prevention of ice/frost formation. In general, the study of the anti-icing and antifogging of superhydrophobic surfaces is just at its beginning stage [109, 110]. Further research is needed to understand the controlling factors to achieve optimized performance. Shen et al. investigate the icephobic property of fluoroalkylsilane (F17)-modified hierarchical Ti6Al4V alloy substrates prepared by the combination of sand blasting and hydrothermal treatment [167]. They concluded that the icing-delay duration of droplets on the superhydrophobic rough Ti6Al4V substrate was many times longer than that of droplets on the smooth hydrophilic substrate, and the ice adhesion strength on superhydrophobic substrate was significantly decreased due to the Cassie state of droplets. Additionally, water droplets always bounced off the superhydrophobic surfaces before freezing under subzero conditions give rise to the promising anti-icing application.

Super-antiwetting layers have also been found to have increased resistance to the microbial-induced corrosion and fouling in sea water due to its capability to reduce bacterial adhesion [168]. Mahalakshmi et al. measured super-antiwetting titanium surface in seawater and found out that microbes did not attach to the surface and the corrosion resistance of titanium in seawater was significantly increased [169].

Metals as important engineering materials are widely used in industrial fields. However, the metal corrosion phenomenon is ubiquitous. Many techniques have been developed to prevent the corrosive process. For example, the use of chromate-containing pigments and paints as protective layers on metal surface for anticorrosion. Concerning the processing and environ-

mental effects, more active techniques should be invented to solve this global corrosion issue. Recently, superhydrophobic surfaces were found to serve as an effective barrier to restrain water, chloride ions, and oxygen from attaching and reacting with the metal surface. For example, Shen et al. fabricated highly hydrophobic TiO_2 nanoparticle films on 316L stainless steel by using a combination of sol-gel and dip-coating process. Even after immersion in an oxygen-saturated Ringer's solution for a duration of 42 days, no metallic oxides are observed in the layers, demonstrating the superior anticorrosion property of such highly hydrophobic TiO_2 coatings [170, 171].

While many techniques have been developed to fabricate superhydrophobic surfaces by creating roughened surfaces and/or changing the surface energy, these techniques are limited by the types of materials to be treated. Our approach can be simply applied to any substrate after the as-prepared highly hydrophobic TNB/FAS powder has dried as a result of the solvent evaporation. To demonstrate the versatility of the current approach, we have also prepared the superhydrophobic porous cross-stacked TNB/FAS structures on a silicon substrate, lab rubber glove, and A4-size printing paper by spraying, spin coating, or dip coating [44]. Figure 12 shows the stable wettability tested through water contact angles under different pH values. This diagram indicated that the as-prepared highly hydrophobic TNB/FAS powder-coated samples remained superhydrophobic with water contact angle larger than 150 ° in a wide pH range from 0 to 14, which suggested that the stable wettability resulted from the high chemical stability of TNB/FAS film over a wide pH range.

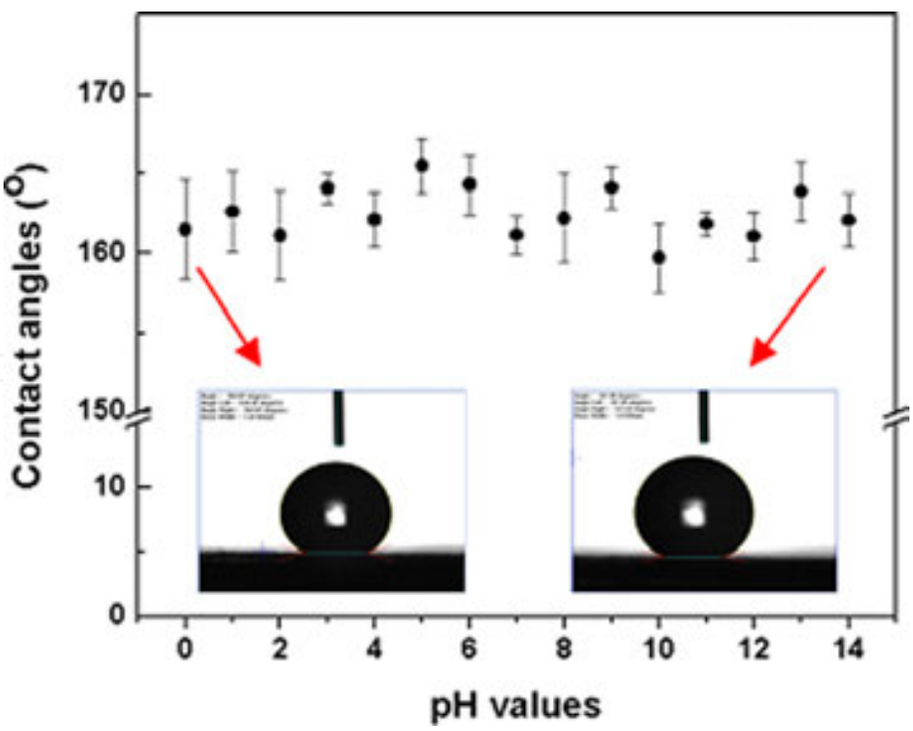

Figure 12. Relationship between pH values and water contact angles of the TNB/FAS films on silicon plate. The contact angle stability indicated that highly hydrophobic TNB/FAS powder coating endowed an excellent anticorrosion property for the coated substrate

http://dx.doi.org/10.5772/60826

3.2.3. Micro-droplet manipulation

The efficient manipulation of micro-droplets offers many potential applications in relation to biomedical and chemical tests and protocols. Super-antiwetting surfaces with in situ controllable/responsive adhesion in a high contrast demonstrate promising applications in micro-droplet manipulation [111-115]. Hence, efforts have also been paid to enhance the transferring process. For example, Jiang et al. prepared high adhesive super-antiwetting polystyrene nanotube layers and used them to catch micro-droplet from super-antiwetting surface with low adhesion. The droplet was then released to a hydrophobic/hydrophilic target [48]. Following this work, they further developed a more effective technique to transfer droplets by the deformation-induced reversible adhesion transition on super-antiwetting polydimethylsiloxane surface [84]. They changed the surface curvature to adjust water droplet adhesion on polydimethylsiloxane pillar array surface from a low adhesive "roll-down" state to a highly adhesive "pinned" state. This provides the possibility for precise, no-loss manipulation of droplets.

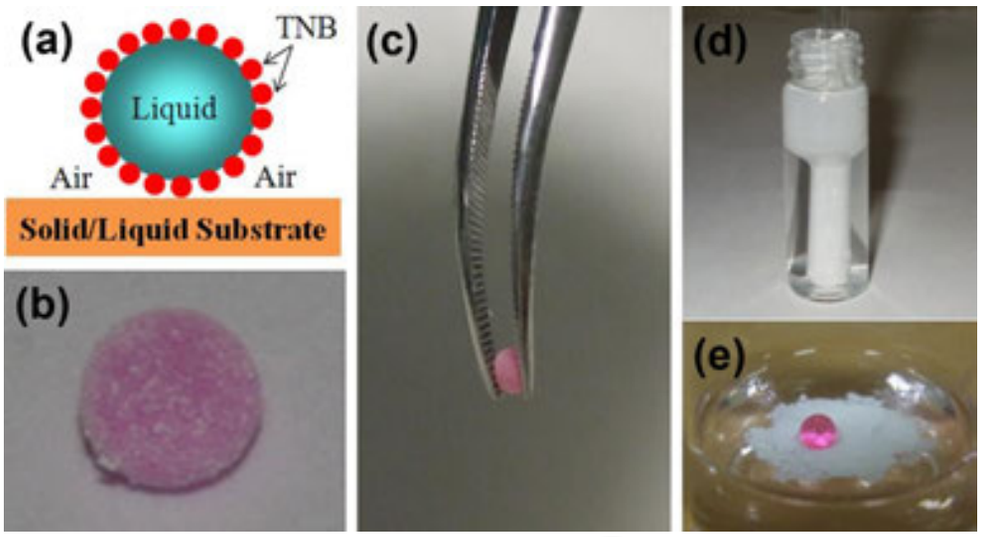

Figure 13. Model (a) and digital image (b) of a liquid marble composed of an RhB colored water droplet coated with TNB/FAS micropowder/nanopowder; (c) images showing a liquid marble being picked up with a pair of tweezers; (d) TNB layer at the air/water interface response to intrusion by a hydrophilic glass stick; and (e) a liquid droplet sitting on the air/liquid interface covered by a layer of highly hydrophobic TNB powder

More interestingly, micro-droplets capsulated by hydrophobic particles to form liquid marbles can be manipulated/transported on various substrates without being contaminated, as shown in Figure 13a, b [44]. The spontaneous encapsulation of TNB/FAS particles around on the water droplet interface is due to the minimization of the free energy of the surface. Another remarkable feature of the marble by such highly hydrophobic titanate nanobelt shell is its strong mechanical strength and high deformability. For example, these marbles can be easily held by a pair of tweezers with large deformation without rupture (Figure 13c). Furthermore, a tightly packed layer self-assembled on liquid surface created a highly robust and flexible superhydrophobic barrier to prevent direct contact between an inserted hydrophilic glass stick and

water solution (Figure 13d). Water droplets larger than 3.0 mm in diameter can also stand on such tightly packed TNB layer (Figure 13e).

3.2.4. Fog, water, and oil collection

In many countries, the spring mornings are graced with spectacular phenomena of dew drops hanging on leaves and on spiders' webs [116-118]. Some plant leaves, in particular, spot particularly large droplets that last well into the morning. Recently, Jiang et al. fully discussed the detailed insights into the directional water collection on spider silk [116]. They discovered that the silk structure made a "wet-rebuilt" change to periodic spindle-knots with random nanofibrils and was separated by joints with aligned nanofibrils after wetting. Guided by the spider silk, they successfully prepared an artificial fiber with a similar structure with the spider silk to realize the directional water collection.

Another example lies with some beetles in the water-limited Namib Desert who collect drinking water from fog-laden wind on their backs [119-122]. Large droplets form by virtue of the insect's bumpy surface which consists of alternating wax-coated hydrophobic and non-waxy hydrophilic regions. Inspired by the water-collecting structure of the desert beetle's back, Cohen et al. fabricated hydrophilic or superhydrophobic patterns on superhydrophobic surfaces with similar fog-collecting characteristics with the desert beetle [120]. Hydrophilic patterns on superhydrophobic surfaces were created with water/2-propanol solutions of a polyelectrolyte to produce surfaces with extreme hydrophobic contrast. Selective deposition of multilayered films onto the hydrophilic patterns introduces different properties to the area.

Recently, inspired by living creatures with special wettability and their precise arrangement of structure and chemical component, we described a facile one-step approach to large-scale construct superamphiphobic TiO_2 film [172]. The as-prepared TiO_2 film displays excellent superamphiphilic property in air, changes to superamphiphobicity with good dynamical stability after silane modification (Figure 14a). Moreover, such superamphiphobic surface reversibly switched from superoleophobic to superoleophilic in air and underwater, respectively (Figure 14b, c). The 3D functional surface would be a versatile platform in a wide range of applications, e.g., self-cleaning, friction reduction, and repeatable water/oil separation. For example, we applied the fluoroalkylsilane-modified pinecone-like TiO_2 particle plates (superoleophobic in air and superoleophilic underwater) as "oil capture hands" to gather oil droplets in water (Figure 14d, process 1-3). The collected oil was then extracted from the water easily to achieve effective oil/water separation (process 4-6). More importantly, it is worth noting that the plate kept self-cleaning without any oil residue due to the excellent superamphiphobic property in air. This is different from the conventional superhydrophobic surface that is completely oil contaminated after oil absorption in water, which makes it difficult for repeated use. This study opens up a new strategy for the treatment of oily wastewater, which has a significant potential for future industrial applications.

3.2.5. Oil/water separation

Oil/water separation technology is very important for a wide range of environmental, agricultural, industrial, and biomedical applications [123-129]. Oil/water separation is a

http://dx.doi.org/10.5772/60826

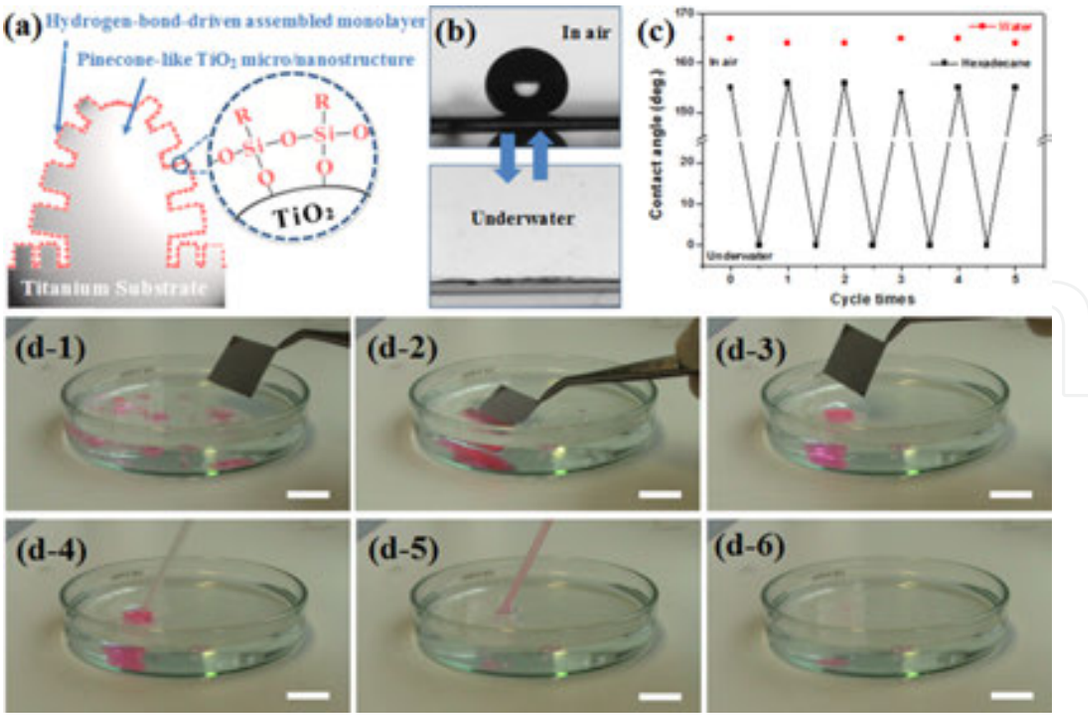

Figure 14. (a) The self-assembled process on the hydroxylated TiO_2 particles surface. (b) The oil droplet image on the modified TiO_2 surface in air or underwater environment. (c) The reversible wetting change of oil droplet on the TiO_2 surface by changing the environment. (d) The oil capture and collection process with a superoleophobic plate. Process 1-3: a superoleophobic plate touches, captures, and collects the sprayed oil drops. Process 4-6: the collected oil droplets are separated from the water. The oil was dyed pink for clear observation of the manipulation process

worldwide challenge due to the increasing industrial oily wastewater and the frequent oil spill accidents. The conventional technique for oil/water separation is dependent on the special porous membranes with both superhydrophobicity and superoleophilicity for the selective separation of oil from the oil/water mixture [123-125]. Ben et al. reported the combination of porous polyurethane and polystyrene microspheres to prepare composite film with highly hydrophobic/oleophilic property for oil/water separation [127]. However, among these approaches and materials used, the fabrication process usually was time consuming, and wettability contrast may decrease under harsh environment. Inspired by the surface geometry and composition of the lotus leaf with its self-cleaning behavior, Huang et al. prepared a TiO_2@fabric composite via a facile strategy for preparing marigold flower-like hierarchical TiO_2 particles through a one-pot hydrothermal reaction [173]. In comparison with hydrophilic cotton fabric, the fluoroalkylsilane (F17)-modified TiO_2@fabric exhibited a high superhydrophobic activity with a contact angle of highly about 160 ° and a sliding angle lower than 10 °. The robust superhydrophobic fabric demonstrated good self-cleaning ability and high efficient oil/water separation due to its extreme wettability contrast of water and oil (Figure 15). Another important water/oil separation process is the preparation of high porous membranes with superoleophilic that can fast absorb oil with high absorption capacity. Stellacci et al. developed a self-assembly process to construct nanowire membranes with high-contrast water/oil wettability [128]. Such superhydrophobic membranes can selectively absorb oils up to 20 times the material's

weight by taking advantage of its high porosity and capillary action. Moreover, the paper-like nanowire membranes demonstrated excellent recyclable separation performance.

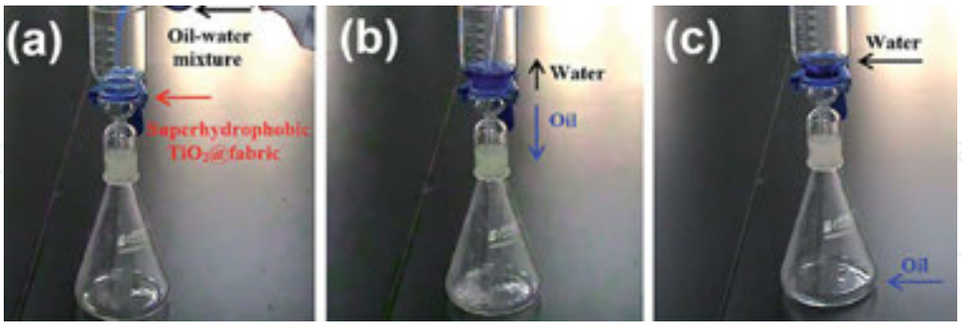

Figure 15. Time sequence of the oil-water separation process with the superhydrophobic F17/TiO_2@fabric

3.2.6. Anti-bioadhesion and biomedical application

Functional TiO_2-based substrates have positive effects in biomedical fields such as biomedical implants, bioactive scaffolds, biosensors, vascular stents, and drug delivery systems [175, 176]. Many factors, such as charge, wettability, composition, and topography, are vital properties for biological applications [176]. Surface with unique wettability is one of the most important items influencing the adsorption of protein and adhesion of platelet, bacteria, and cell [130-139]. Antiwetting surfaces, both smooth and having suitable surface roughness of varying length scales to create super-antiwetting, were incubated in protein solution. The samples were then exposed to flow shear in a device designed to simulate a microfluidic environment. It is reported that a similar amount of protein adsorbed onto smooth and nanometer-scale rough surfaces with static incubation, although a greater amount was found to adsorb onto super-antiwetting surfaces with micrometer-scale roughness, resulted from the increasing binding strength of hydrophobic interactions between bovine serum albumin and the super-antiwetting surface. However, incubated in a flow cell similar to that used in microfluidics, flow shear removed a considerably larger proportion of adsorbed protein from the super-antiwetting surfaces than from the smooth ones, with almost all of the protein being removed from some nanoscaled surfaces. This type of surface may therefore be useful in microfluidics, where protein sticking is a problem. Moreover, they reported that super-antiwetting surfaces with larger roughness dimensions (~4 μm or 800 nm particle size) caused increased adsorption of protein than the copper oxide nano-pillars about 60 nm wide and 10 nm thick.

Platelet attachment and activation on biomedical implant surfaces may lead to blood coagulation and thrombosis. Therefore, regulating the surface wettability to increase the blood compatibility is an effective way for the decrease of platelet adhesion. Recently, Lin et al. [132] studied the effect of surface energy on TiO_2 on antiplatelet activity. The in vitro blood compatibility experiment indicated that the super-antiwetting nanotube TiO_2 layers exhibit a remarkable ability in reducing platelet adhesion (Figure 16c). Compared to the relatively high amount of platelets on superhydrophilic TiO_2 nanotube surface (Figure 16b, 22 ± 1.5 per 5,

http://dx.doi.org/10.5772/60826

000μm²) and flat Ti surface (Figure 16a, 77 ± 7.4 per 5, 000 μm²), only very few platelets (1 ± 0.8 per 5, 000 μm²) were found to adhere on the super-antiwetting TiO_2 nanotube layers. Moreover, even though some platelets were occasionally attached to the super-antiwetting surface, they looked smooth without any growth of pseudopods, implying that the platelets adhered on the super-antiwetting TiO_2 nanotube surface remain inactive and hardly grow and spread out. From the in vitro evaluation, the super-antiwetting TiO_2 nanotube layers exhibited excellent blood compatibility and remarkable performance in preventing platelets from adhering to the implant surface. Tang et al. also observed the similar bacterial adhesion on TiO_2 structures with various surface wettabilities [177]. Compared to ordinary hydrophilic or hydrophobic film, the as-prepared superhydrophobic structured film can greatly decrease the adhesion and activation of *Staphylococcus aureus*. This indicates that the special topography and wettability play critical role in blood compatibility.

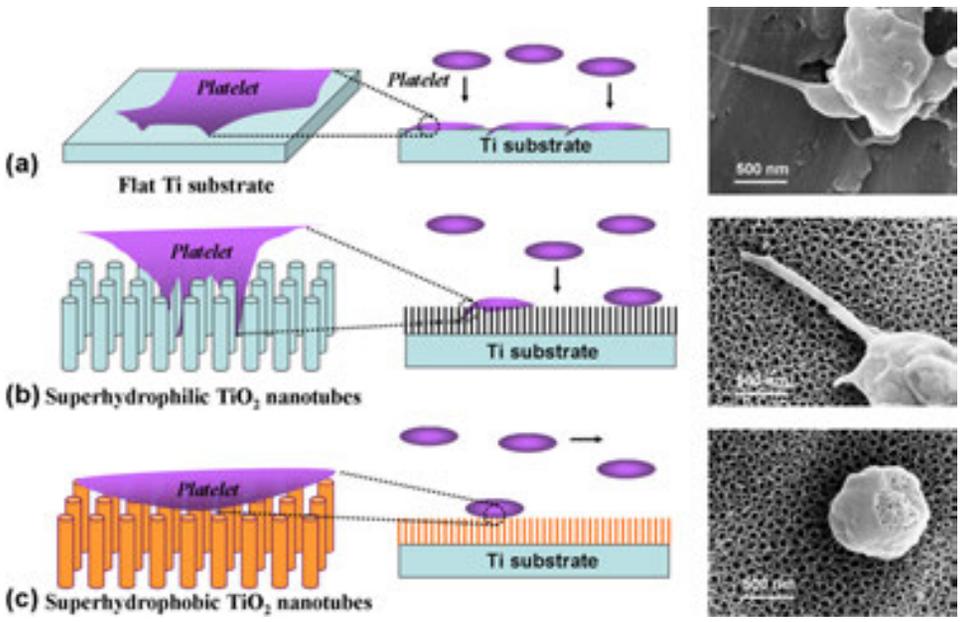

Figure 16. Schematic illustration of the morphology of platelets and their interactions with different wetting surfaces. (a) Plain Ti substrate; (b) superhydrophilic TiO_2 nanotubes; (c) superhydrophobic TiO_2 nanotubes

3.2.7. Friction reduction

The transportation of a liquid through a conventional smooth pipe or tube is dominated by the frictional drag on the liquid against the walls. In general, an air layer at or near the boundary between the solid and liquid, achieved by producing bubbles at the interface, by the vaporization of liquid or by a cushion of air (e.g., below a hovercraft), can reduce the resistance to flow against a solid. However, these methods require a continuous energy consumption. Recently, nonstick super-antiwetting surfaces demonstrating high static contact angles, low contact area, and lateral friction to liquid droplets on natural surfaces have attracted much attention of researchers [156-165]. Watanabe and Zou et al. described a more reduced flow adhesion and friction phenomena when water is passed through a super-antiwetting surface

in comparison to lower antiwetting surfaces [155, 156]. The flow resistance reduction is attributed to the reduced molecular attraction and the resultant solid/liquid contact area by the air layer trapped in the rough microstructured/nanostructured super-antiwetting surfaces. To the best of our knowledge, most reports used small sections of lithographically patterned substrates and rarely considered the pressure contrasts or varying flow rates. McHale et al. found that the super-antiwetting nanoribbon coating allowed greater flow at low pressure differences, but the effect on friction reduction disappeared as the pressure increased [158]. Large pressure and friction forces are known to be detrimental in microelectromechanical system applications due to large surface-to-volume ratio and minute spacing [160, 161].

3.3. Super-wetting/antiwetting TiO_2-based surfaces

Titanium dioxide (TiO_2), as another active ingredient for self-cleaning and forming superhydrophobic surfaces, has been widely employed in recent years. By constructing a TiO_2 film and modifying the resultant film with low-surface-energy fluoroalkylsilane molecules, a super-antiwetting TiO_2 film would be easily fabricated with additional photo-patternable properties. Such uniform film was able to be conveniently patterned with ultraviolet light to one-step create super-wetting/antiwetting surface micropatterns. Precise adjustment over the chemistry and geometry of functional materials based on patterned template with highly wetting contrast is of significant importance for a wide range of applications. For example, the wetting pattern could be utilized to site specifically immobilized biomolecules, and metal or semiconductor particles, for multifunctional applications.

3.3.1. Template for micropatterning/printing

It is still a primary challenge for uniform assembling functional inorganic nanomaterials. In this project, nature smartly adopts a perfect approach in biomineralization, where "matrix" macromolecules induce nucleation and growth of inorganic crystals at specific positions with controlled shape, size, morphology, and even orientation. Recently, patterned thin films had received considerable attention due to their interesting properties for widely potential applications [178, 179]. Compared to the traditional patterning techniques of physical/chemical vapor deposition or sputtering, solution-based deposition approaches are becoming popular for the patterning films creation due to the facile synthesis parameters and conditions, less energy, and time requirement [180, 181]. Although the common photolithographic patterning technique is excellent for preparing submicron-sized template in solution, it is a complex multistep process that has to remove great part of the formed film and the supplemental photoresist [182]. Super-wetting/antiwetting pattern with an extreme wettability contrast by photolithography, particularly the rewritable pattern by using high photocatalytic activity of anatase TiO_2 [140-144], is a potentially powerful and economical approach to precisely construct various multifunctional nanostructures in aqueous solution [145-149]. However, such photolithography technique require high-energy light sources of X-ray or laser and ultrahigh vacuum to directly destroy the low-energy materials to some extent or only suitable for semiconductor substrate with inherent photocatalytic activity. For example, Li et al. applied femtosecond laser to one-step construct a three-dimensional (3D) on-demand wettability

http://dx.doi.org/10.5772/60826

pattern on a superhydrophobic surface (Figure 17) [175]. We also demonstrated that 3D binary pattern with extremely high contrast would be applied as microfluidic manipulators and biomedical scaffolds to guide droplet transportation and cell site-selective growth, respectively. Moreover, the wetting patterns prepared by UV photocatalytic decomposed surface low-energy groups or monolayer is invisible under ambient condition [94]. Such highly contrast wetting patterns would be developed or exposed under a certain condition (Figure 18), e.g., humid air atmosphere, underwater, fluororesin labeling, and solvent site-selective assembling.

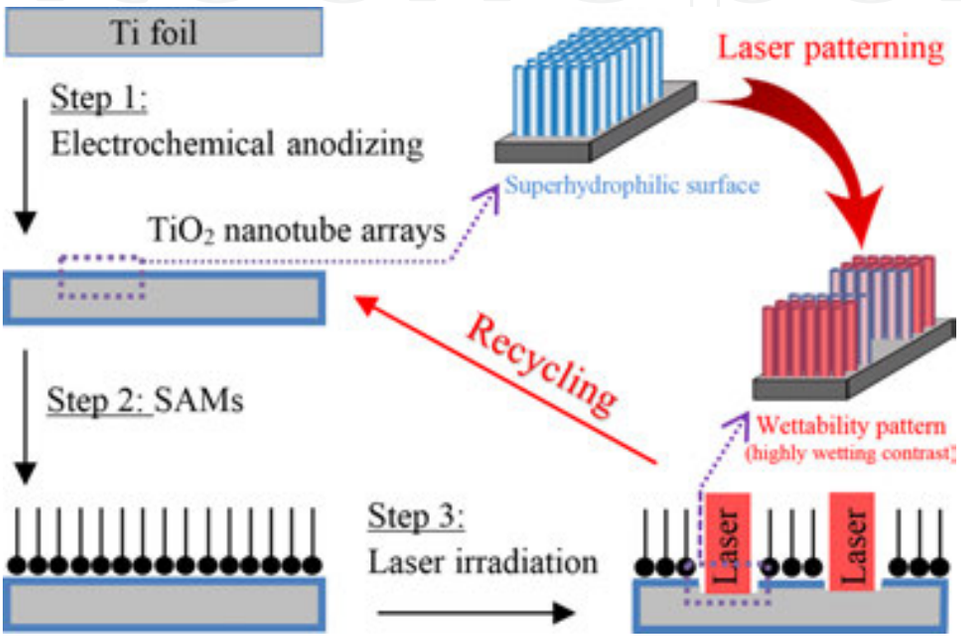

Figure 17. Schematic outline of the procedures to construct superhydrophilic-superhydrophobic micropattern by an ultrafast laser processing technique

Based on ink patterning template with an extreme wettability, adhesion, and conduction contrast (superamphiphobic/amphiphilic), we develop versatile patterning strategies without the requirement of seed/catalyst to construct shape-controlled (positive/negative) ZnO nanomaterial patterns [94]. Specifically, ZnO nanorods are site-selective deposited by a facile liquid-phase deposition process on the ink covering regions to prepare a positive micropattern with clear boundaries (Figure 19a). The obvious suppression phenomenon in superamphiphobic regions is ascribed to the air pocket trapped between the liquid solution and superamphiphobic substrate to highly inhibit the direct solid/liquid interaction. By taking advantage of ink coating with nonconducting character, we realize the rapid construction of an unconventional negative ZnO micropattern on the superamphiphobic regions instead of the superamphilphic regions under the assistance of electric field (Figure 19b). Such wetting micropattern with a high contrast by ink-printing technique is particularly useful and promising in constructing dual-scale or even complicate nanostructures optoelectronic device on a large scale, e.g., photodetectors and photo-sensors.

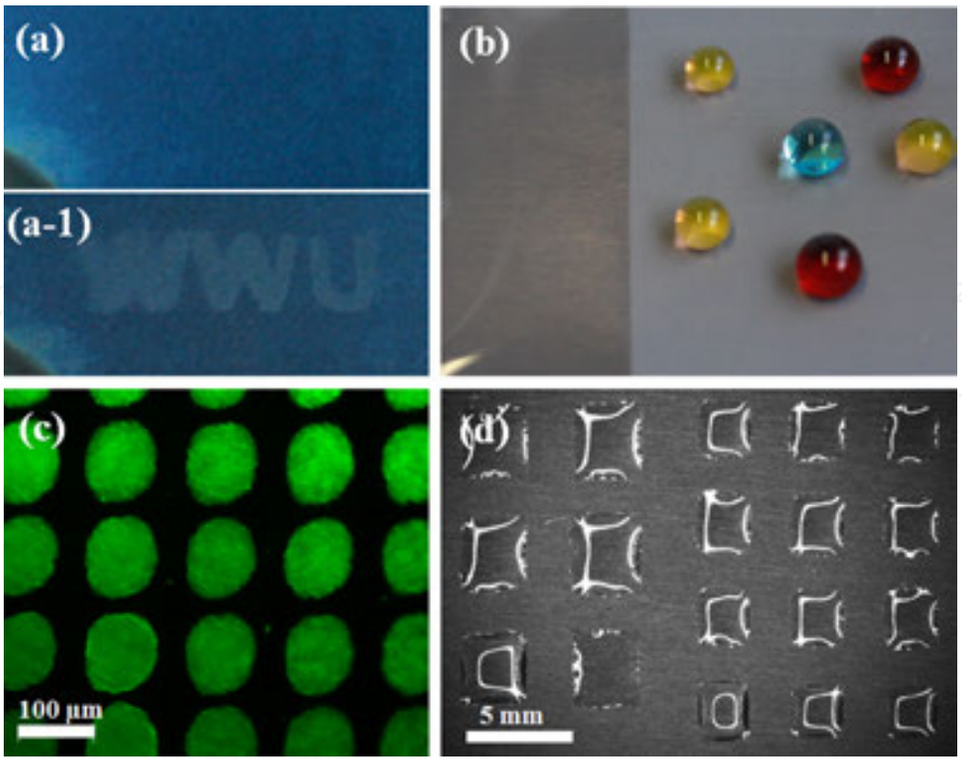

Figure 18. (a) Optical image of an invisible pattern on a superamphiphobic surface constructed by a photo-cleavage strategy and (a-1) the exposed image of "WWU" under humid air atmosphere. Typical wetting patterns exposed with (b) water wetting, (c) fluororesin labeling, and (d) site-selective solvent assembling

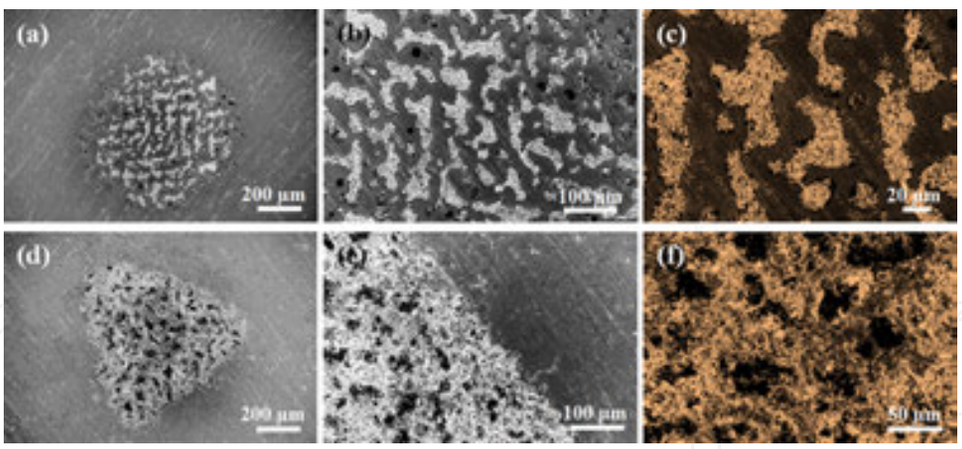

Figure 19. FESEM images of ZnO nanoparticles deposited on ink-patterned superamphiphobic TiO_2 surface. (a-c) Site-selective deposition of ZnO nanoparticles on ink-covered areas by a wet chemical deposition technique to form a positive pattern; (d-f) site-selective deposition on ink-free regions by an electrochemical technique to create a contrary negative pattern

On the basis of photolithography patterning technique on TiO_2 structures, we applied the as-prepared two-dimensional (2D) superhydrophilic-superhydrophobic pattern as scaffold to direct and guide the selective attachment of cell for high-throughput cell behavior evaluation, bioassay, and other related applications (Figure 20) [183]. Following this principle, arrays of

http://dx.doi.org/10.5772/60826

TiO_2 [149], ZnO [150], crystalline CdS materials [151], molecular probes [152], and bioactive CaP layer [153] were nucleated and assembled directly from solution onto Ti substrates at the desired locations precisely. Such patterned structures can then be fabricated into matrix devices for large-scale microelectronic applications or bio-compatible coatings where drugs could be encapsulated in specific regions of the coating [154]. This strategy for micropatterned composites will be helpful to develop various micropatterned functional nanostructured materials. However, a big challenge for widespread practical applications remains to be the development of high-throughput, low-cost, and easily controlled techniques to achieve desired orientation of the nanoscale units.

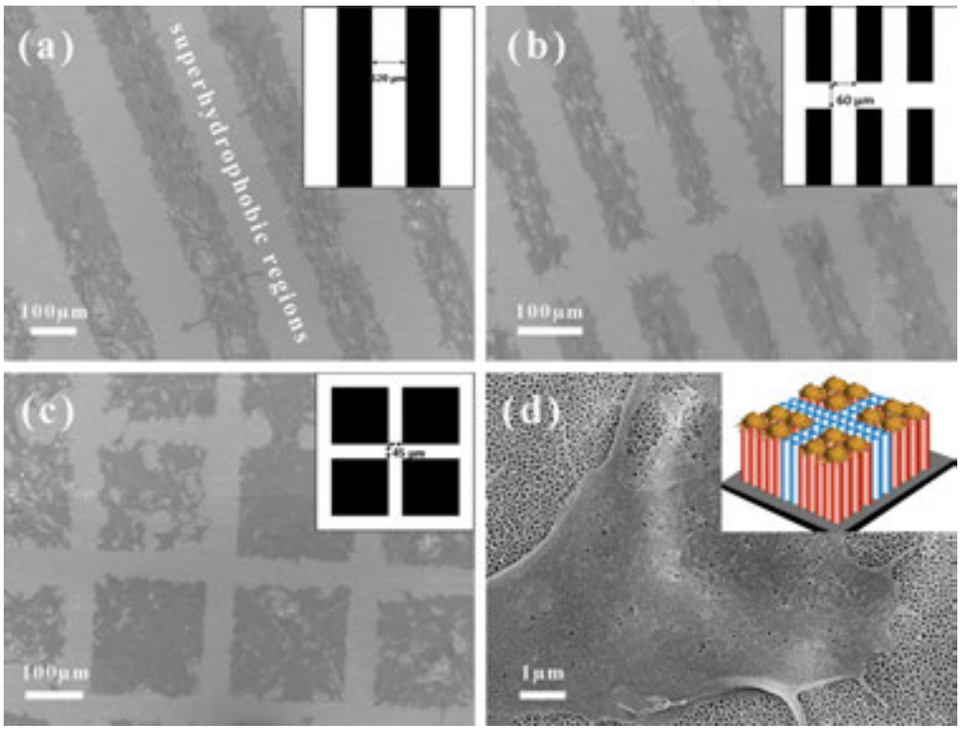

Figure 20. (a-c) SEM images of 3T3 cell adhesion on the super-antiwetting micropatterns with various shapes and sizes. (d) Magnified image of cell on super-wetting region and the schematic diagram of the site-selective cell attachment on scaffold

3.3.2. Molecular sensing device

A biosensor is a device incorporating specific molecular recognition on the basis of the affinity between sensing units and targeted enzyme, antibody or molecular. The novel dual micro-nanoscale patterning surfaces described in previous sections have a wide range of potential applications. As an example, Lai et al. investigated the surface-enhanced Raman scattering (SERS) sensing property of the silver nanoparticles (AgNP) decoration on TiO_2 patterns with a electrodeposition process (Figure 21a, b) [183]. Using rhodamine 6G probing molecule, the patterned AgNP@TiO_2 sample displays an excellent SERS effect with a high SERS contrast between superhydrophilic and superhydrophobic areas (Figure 21c). The AgNPs within the superhydrophilic areas exhibited an obvious and uniform SERS enhancement. This is ascribed

to the novel 3D rough structure TiO_2 substrate with a high surface area for high-density loading of AgNPs and absorption of probing molecules. On the contrary, the SERS intensity was negligible at the superhydrophobic areas. This is attributed to the fact that an air pocket at the solid/liquid interface has a strong resistance for AgNPs coating and rhodamine 6G loading in the superhydrophobic areas. Furthermore, based on the high efficient photocatalytic ability of anatase TiO_2 on neat superhydrophilic SERS substrate, the AgNP@TiO_2 can be obtained by rapidly decomposing the absorbed organic molecules into inorganic molecules, such as H_2O and CO_2 (Figure 21d). Such recyclable micropatterned AgNP@TiO_2 devices, by taking advantage of high contrast wettability of TiO_2 patterns, can be a highly sensitive and reproducible SERS sensor candidate for high-throughput molecules detection and biorecognition.

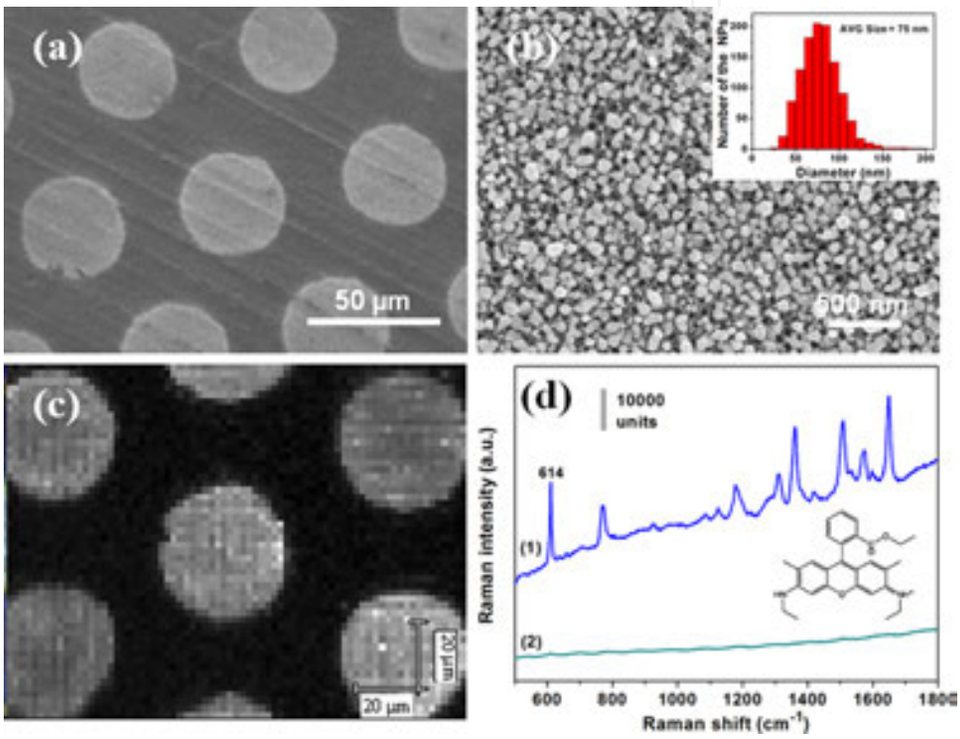

Figure 21. SEM image of AgNP@TiO_2 micropattern (a) and the corresponding magnified view of Ag particles assembled on the superhydrophilic areas (b). SERS mapping of AgNP@TiO_2 pattern with a rhodamine 6G probe using the reference peak of 614 cm^{-1} (c). (d) Raman spectra of the rhodamine 6G molecules loaded on AgNP@TiO_2 with (2) or without UV irradiation (1). The inset of (b) shows the corresponding AgNP size distribution

3.3.3. Microfluidic manipulation

As discussed above, most of wetting patterns are invisible and require to develop under certain conditions, e.g., fluororesin/solvent labeling, underwater, or humid environment. Recently, we reported a facile and in situ bottom-up surface modification method to create high-surface-energy ink patterning on superhydrophobic TiO_2 substrates by pen drawing or using commercially available desktop printing technology [70]. Such one-step bottom-up process can realize the simultaneous adjustment of surface topography and chemical component to obtain visible wetting patterns with extremely high adhesion contract. The visible tunability of the superhydrophobic surface wetting and adhesion are suitable to implement four basic opera-

http://dx.doi.org/10.5772/60826

tions for the manipulation of liquid drops from storage, transfer, transport, and mixing (Figure 22). In their two-dimensional lab-on-paper prototype, liquid droplets adhere to the porous substrate, rather than absorbing into the substrate; as a result, liquid droplets remain accessible for further quantitative testing and analysis after performing simple qualitative on-chip testing.

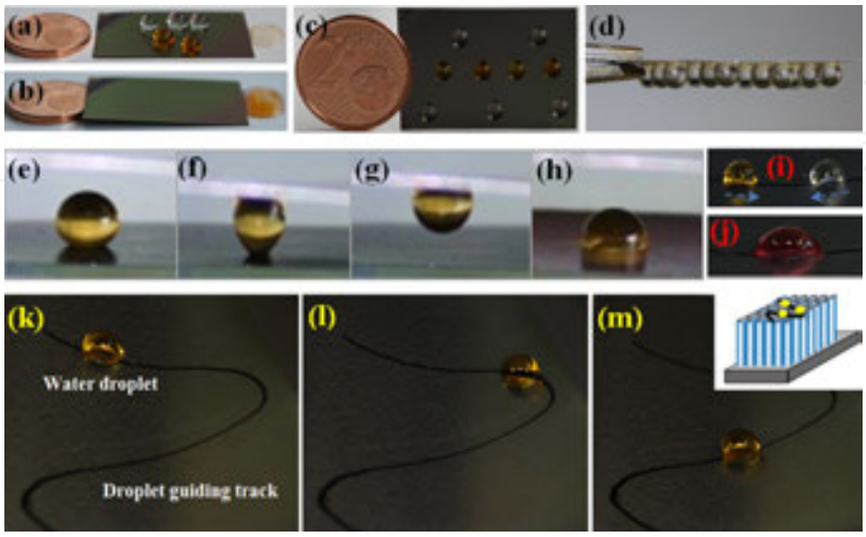

Figure 22. The uncontrollable and unstable liquid droplets on uniform superhydrophobic TNA surface (a, b). Implementation of adhesion contrast on some typical micro-droplet manipulation processes based on the ink-patterned superhydrophobic TNA surfaces: storage (c, d), transfer (e-h), mixing (i, j), and collection (k-m)

4. Summary and outlook

Despite the insightful studies and many promising applications of nanostructures with special wettability and adhesion, great challenges still remain in applying them in practical applications [184]. For example, TiO_2-based surfaces tend to lose their super-wetting ability on a cloudy day or in the dark because the photo-induced superhydrophilic ability of TiO_2 is mainly active with UV light. The photo-induced super-wetting TiO_2 surfaces will recover to a more hydrophobic level within minutes to hours, which restricts their practical applications in our daily life. To construct super-wetting TiO_2-based surfaces without the requirement of UV illumination, various synthesis processes or modification techniques should been developed to prepare visible light active TiO_2-based surfaces in the future. As above stated, a micro-/nano-surface roughness and a low surface energy is prerequisite for super-antiwetting; thus, they generally suffer from weak durability due to the mechanically fragile hierarchical structure, and the rapid degradation of surface functional chemistry resulted from the high photocatalytic activity of anatase TiO_2. Any damage of the micro-/nano-topographical structures or the loss of the low-surface-energy layer may result in a reduction of its super-antiwetting ability. Although extensive studies have been carried out, developing processes to create superhydrophobic surfaces, research on the durability aspect of superhydrophobic surface only started a few years ago. Several concepts to improve the mechanical durability of superhydrophobic surfaces are suggested, for example, by using hierarchical roughness in which robust micro-

scale bumps can provide protection to the more fragile nanoscale roughness, using 3D uniform buck materials and incorporating self-healing materials.

The chapter reviews the recent advance on the natural and bio-inspired super-antiwetting surfaces with different kinds of special adhesion properties, such as low adhesion, high adhesion, anisotropic adhesion, and stimuli-responsive adhesion. Studies on the biological structure surfaces and the biomimetic fabrication of artificial surfaces reveal that the combination of topography structure and chemical component results in these special adhesion states. For example, the tailoring of topography and the scale of microstructures and nanostructures to achieve certain contact models can effectively change the solid/liquid adhesion from low to high levels. On the other hand, the specific arrangement of the microstructures and the chemical component may result in anisotropic solid/liquid adhesion. Furthermore, reversible switching of adhesion between the low-adhesive rolling state and high-adhesive pinning state for water droplets on a superhydrophobic surface could be achieved via cooperation of the stimuli-responsive materials and surface roughness. In addition, potential applications of super-antiwetting surfaces with special adhesion were also discussed, including self-cleaning, water/oil separation, microfluidic manipulation, and micro-templates.

Super-antiwetting surface with responsive liquid adhesion has attracted much attention; great progress has been achieved recently. However, up to now, most adhesion changes reported are achieved ex situ, which require a different droplet to study the adhesion on smart responsive surfaces. Many problems, such as stability and cost of materials with multifunctionalities, need to be addressed before industrial applications can be realized. Therefore, stable, renewable, and smart responsive super-antiwetting surface with solid/liquid adhesion adjustment in a high contrast under single or multiple stimuli responses is a key issue for future investigation. Moreover, the in situ and fast adhesive force measurement on the super-antiwetting substrates is still needed to be improved.

Acknowledgements

The authors thank the Natural Science Foundation of Jiangsu Province of China (BK20130313; BK20140400), and Priority Academic Program Development of Jiangsu Higher Education Institutions (PAPD) for financial support of this work.

Author details

Jian-Ying Huang and Yue-Kun Lai*

*Address all correspondence to: yklai@suda.edu.cn

National Engineering Laboratory for Modern Silk, College of Textile and Clothing Engineering, Soochow University, Suzhou, China

References

[1] Liu KS, Yao X, Jiang L. Chem. Rev. 2015; 114: 10044.

[2] Feng L, Li SH, Li YS, Li HJ, Zhang LJ, Zhai J, Song YL, Liu BQ, Jiang L, Zhu DB. Adv. Mater. 2002; 14: 1857.

[3] Lafuma A, Quéré D. Nat. Mater. 2003; 2: 457.

[4] Sun TL, Feng L, Gao XF, Jiang L. Acc. Chem. Res. 2005; 38: 644.

[5] Feng XJ, Jiang L. Adv. Mater. 2006; 18: 3063.

[6] Roach P, Shirtcliffe NJ. Newton MI. Soft Matter 2008; 4: 224.

[7] Xia F, Jiang L. Adv. Mater. 2009; 20: 2842.

[8] Zhu H, Guo ZG, Liu WM. Chem. Commun. 2014; 50: 3900.

[9] Xin BW, Hao JC, Chem. Soc. Rev. 2010; 39: 769.

[10] Teisala H, Tuominen M, Kuusipalo J. Adv. Mater. Interface 2014; 1: 1300026.

[11] Guo ZG, Liu WM, Su BL. J. Colloid Interface Sci. 2011; 353: 335.

[12] del Campo A, Arzt E. Chem. Rev. 2008; 108: 911.

[13] Darmanin T, de Givenchy ET, Amigoni S, Guittard F. Adv. Mater. 2013; 25: 1378.

[14] Wang XF, Ding B, Yu JY, Wang MR. Nano Today 2011; 6: 510.

[15] Liu MJ, Zheng YM, Zhai J, Jiang L. Acc. Chem. Res. 2010; 43: 368.

[16] Bhushan B, Jung YC. Prog. Mater. Sci. 2011; 56: 1.

[17] Wang S, Jiang L. Adv. Mater. 2007; 19: 3423.

[18] Wenzel RN. Ind. Eng. Chem. 1936; 28: 988.

[19] Cassie ABD, Baxter S. Trans. Faraday Soc. 1944; 40: 546.

[20] Wang R, Hashimoto K, Fujishima A, Chikuni M, Kojima E, Kitamura A, Shimohigoshi M, Watanabe T. Nature 1997; 388: 431.

[21] Fujishima A, Zhang XT, Tryk DA. Surf. Sci. Rep. 2008; 63: 515.

[22] Zhang XT, Fujishima A, Jin M, Emeline AV, Murakami T. J. Phys. Chem. B 2006; 110: 25142.

[23] Li Q, Shang JK. Environ. Sci. Technol. 2010; 44: 3493.

[24] Mugele F, Baret JC. J. Phys. Condens. Matter. 2005; 17: R705.

[25] Ma CF, Nagai A, Yamazaki Y, Toyama T, Tsutsumi Y, Hanawa T, Wang W, Yamashita K. Acta Biomater. 2012; 8: 860.

[26] Meng FM, Xiao L, Sun ZQ. J. Alloys Compd. 2009; 485: 848.

[27] Lai YK, Chen YC, Tang YX, Gong GG, Chen Z, Lin CJ. Electrochem. Commun. 2009; 11: 2268.

[28] Song S, Jing LQ, Li SD, Fu HG, Luan YB. Mater. Lett. 2008; 62: 3503.

[29] Funakoshi K, Nonami T. J. Am. Ceram. Soc. 2006; 89: 2782.

[30] Xi BJ, Verma LK, Li J, Bhatia CS, Danner AJ, Yang H, Zeng HC. ACS Appl. Mater. Interfaces 2012; 4: 1093.

[31] Liu KS, Zhang ML, Zhai J, Wang J, Jiang L. Appl. Phys. Lett. 2008; 92: 183103.

[32] Gao XF, Jiang L. Nature 2004; 432: 36.

[33] Guo ZG, Zhou F, Hao JC, Liu WM. J. Am. Chem. Soc. 2005; 127: 15670.

[34] Xi JM, Feng L, Jiang L. Appl. Phys. Lett. 2008; 92: 053102.

[35] Nosonovsky M, Bhushan B. Curr. Opin. Colloid Interface Sci. 2009; 14: 270.

[36] Tuteja A, Choi W, Ma ML, Mabry JM, Mazzella SA, Rutledge GC, McKinley GH, Cohen RE. Science 2007; 318: 1618.

[37] Wang DA, Wang XL, Liu XJ, Zhou F. J. Phys. Chem. C 2010; 114: 9938.

[38] Bhushan B, Jung YC, Niemietz A, Koch K. Langmuir 2009; 25: 1659.

[39] Xie QD, Xu J, Feng L, Jiang L, Tang WH, Luo XD, Han CC. Adv. Mater. 2004; 16: 302.

[40] Meng HF, Wang ST, Xi JM, Tang ZY, Jiang L. J. Phys. Chem. C 2008; 112: 11454.

[41] Koch K. Bhushan B. Jung YC, Barthlott W. Soft Matter 2009; 5: 1386.

[42] Wu WC, Wang XL, Wang DA, Chen M, Zhou F, Liu WM, Xue QJ. Chem. Commun. 2009; 9: 1043.

[43] Yao X, Chen QW, Xu L, Li QK, Song YL, Gao XF, Quéré D, Jiang L. Adv. Funct. Mater. 2010; 20: 656.

[44] Lai YK, Tang YX, Huang JY, Wang H, Li HQ, Gong DG, Ji XB, Gong JJ, Lin CJ, Sun L, Chen Z. Soft Matter 2011; 7: 6313.

[45] Autumn K, Liang YA, Hsieh ST, Zesch W, Chan WP, Kenny TW, Fearing R, Full RJ. Nature 2000; 405: 681.

[46] Bhushan B, Her EK. Langmuir 2010; 26: 8207.

[47] Feng L, Zhang YA., Xi JM, Zhu Y, Wang N, Xia F, Jiang L. Langmuir 2008; 24: 4114.

[48] Jin MH, Feng XJ, Xi JM, Zhai J, Cho KW, Feng L, Jiang L. Macromol. Rapid Commun. 2005; 26: 1805.

[49] Guo ZG, Liu WM. Appl. Phys. Lett. 2007; 90: 223111.

[50] Boscher ND, Carmalt CJ, Parkin IP. J. Mater. Chem. 2006; 16: 122.

[51] Zhao WJ, Wang LP, Xue QJ. J. Phys. Chem. C 2010; 114: 11509.

[52] Park SG, Moon HH, Lee SK, Shim J, Yang SM. Langmuir 2010; 26: 1468.

[53] Zhu SJ, Li YF, Zhang JH, Lu CL, Dai X, Jia F, Gao HN, Yang BJ. Colloid Interface Sci. 2010; 344: 541.

[54] Lai YK, Gao XF, Zhuang HF, Huang JY, Lin CJ, Jiang L. Adv. Mater. 2009; 21: 3799.

[55] Farsinezhad S, Waghmare PR, Wiltshire BD, Sharma H, Amiri S, Mitra SK, Shankar K. RSC Adv. 2014; 4: 33587.

[56] Cheng ZJ, Gao J, Jiang L. Langmuir 2010; 26: 8233.

[57] Gao LC, McCarthy TJ, Zhang X. Langmuir 2009; 25: 14100.

[58] Balu B, Kim JS, Breedveld V, Hess DW. J. Adhesion Sci. Technol. 2009; 23: 361.

[59] Ting WH, Chen CC, Dai SA, Suen SY, Yang IK, Liu L, Chen FMC, Jeng RJ. J. Mater. Chem. 2009; 19: 4819.

[60] Park BG, Lee W, Kim JS, Lee KB. Colloids Surf. A 2010; 370: 15.

[61] Lee W, Park BG, Kim DH, Ahn DJ, Park Y, Lee SH, Lee KB. Langmuir 2010; 26: 1412.

[62] Lai YK, Lin CJ, Huang JY, Zhuang HF, Sun L, Nguyen T. Langmuir 2008; 24: 3867.

[63] Di Mundo R, Palumbo F, d'Agostino R. Langmuir 2010; 26: 5196.

[64] Sun W, Shen LY, Wang LM, Fu K, Ji J. Langmuir 2010; 26: 14236.

[65] Huang JY, Lai YK, Wang LN, Li SH, Ge MZ, Zhang KQ, Fuchs H, Chi LF. J. Mater. Chem. A 2014; 2: 18531.

[66] Yang J, Zhang ZZ, Men XH, Xu XH, Zhu XT. J. Colloid Interface Sci. 2010; 346: 241.

[67] Wang DA, Liu Y, Liu XJ, Zhou F, Liu WM, Xue QJ. Chem. Commun. 2009; 45: 7018.

[68] Liu XJ, Ye Q, Yu B, Liang YM, Liu WM, Zhou F. Langmuir 2010; 26: 12377.

[69] Liu XJ, Wu WC, Wang XL, Luo ZZ, Liang YM, Zhou F. Soft Matter 2009; 5: 3097.

[70] Lai YK, Pan F, Xu C, Fuchs H, Chi LF. Adv. Mater. 2013; 25: 1682.

[71] Zhang LB, Wu JB, Hedhili MN, Yang XL, Wang P. J. Mater. Chem. A 2015; 3: 2844.

[72] Nishimoto S, Becchaku M, Kameshima Y, Shirosaki Y, Hayakawa S, Osaka A, Miyake M. Thin Solid Films 2014; 558: 221.

[73] Xu QF, Liu Y, Lin FJ, Mondal B, Lyons AM. ACS Appl. Mater. Interface 2013; 5: 8915.

[74] Uchida K, Nishikawa N, Izumi N, Yamazoe S, Mayama H, Kojima Y, Yokojima S, Nakamura S, Tsujii K, Irie M. Angew. Chem. Int. Ed. 2010; 49: 5942.

[75] Xu L, Ye Q, Lu X. Lu Q. ACS Appl. Mater. Interfaces 2014; 6: 14736.

[76] Zhao XD, Fan M, Luo J, Ding J, Liu XY, Zou BS, Feng YP. Adv. Funct. Mater. 2011; 21: 184.

[77] Liu MJ, Nie FQ, Wei ZX, Song YL, Jiang L. Langmuir 2010; 26: 3993.

[78] Verplanck N, Galopin E, Camart JC, Thomy V, Coffinier Y, Boukherroub R. Nano Lett. 2007; 7: 813.

[79] Lapierre F, Thomy V, Coffinier Y, Blossey R, Boukherroub R. Langmuir 2009; 25: 6551.

[80] Li C, Guo RW, Jiang X, Hu SX, Li L, Cao XY, Yang H, Song YL, Ma YM, Jiang L. Adv. Mater. 2009; 21: 4254.

[81] Chen L, Liu MJ, Lin L, Zhang T, Ma J, Song YL, Jiang L. Soft Matter 2010; 6: 2708.

[82] Hong X, Gao X, Jiang L. J. Am. Chem. Soc. 2007; 129: 1478.

[83] Cheng ZJ, Feng L, Jiang L. Adv. Funct. Mater. 2008; 18: 3219.

[84] Wu D, Wu SZ, Chen QD, Zhang YL, Yao J, Yao X, Niu LG, Wang JN, Jiang L, Sun HB. Adv. Mater. 2011; 23: 545.

[85] Zhang JL, Lu XY, Huang WH, Han YC. Macromol. Rapid Commun. 2005; 26: 477.

[86] Zhang QL, Xia F, Sun TL, Song WL, Zhao TY, Liu MC, Jiang L. Chem. Commun. 2008; 10: 1199.

[87] Tian D, Chen Q, Nie FQ, Xu JJ, Song YL, Jiang L. Adv. Mater. 2009; 21: 3744.

[88] Xia F, Ge H, Hou Y, Sun TL, Chen L, Zhang GZ, Jiang L. Adv. Mater. 2007; 19: 2520.

[89] Xu LY, Lu XM, Li M, Lu QH. Adv. Mater. Interfaces 2014; 1: 1400011.

[90] Wang DA, Liu Y, Liu XJ, Zhou F, Liu WM, Xue QJ. Chem. Commun. 2009; 45: 7018.

[91] Zheng YM, Gao XF, Jiang L. Soft Matter 2007; 3: 178.

[92] Chen Y, He B, Lee JH, Patankar NA. J. Colloid Interface Sci. 2005; 281: 458.

[93] Gao XF, Yao X, Jiang L. Langmuir 2007; 23: 4886.

[94] Huang JY, Lai YK, Pan F, Yang L, Wang H, Zhang KQ, Fuchs H, Chi LF. Small 2014; 10: 4865.

[95] Furstner R, Barthlott W, Neinhuis C, Walzel P. Langmuir 2005; 21: 956.

[96] Nakajima A, Hashimoto K, Watanabe T, Takai K, Yamauchi G, Fujishima A. Langmuir 2000; 16: 7044.

[97] Bhushan B, Jung YC, Koch K. Langmuir 2009; 25: 3240.

[98] Qi DP, Lu N, Xu HB, Yang BJ, Huang CY, Xu MJ, Gao LG, Wang ZX, Chi LF. Langmuir 2009; 25: 7769.

[99] Nystrom D, Lindqvist J, Ostmark E, Antoni P, Carlmark A, Hult A, Malmstrom E. ACS Appl. Mater. Interface 2009; 1: 816.

[100] Xiu YH, Hess DW, Wong CP, J. Adhes. Sci. Technol. 2008; 22: 1907.

[101] Mishchenko L, Hatton B, Bahadur V, Taylor JA, Krupenkin T, Aizenberg J. ACS Nano 2010; 4: 7699.

[102] Kulinich SA, Farhadi S, Nose K, Du XW. Langmuir 2011; 27: 25.

[103] Cao LL, Jones AK, Sikka VK, Wu JZ, Gao D. Langmuir 2009; 25: 12444.

[104] Z. L. Liu, Y. J. Gou, Wang JT, Cheng SY. Int. J. Heat Mass. Tran. 2008; 51: 5975.

[105] Gao XF, Yan X, Yao X, Xu L, Zhang K, Zhang JH, Yang B, Jiang L. Adv. Mater. 2007; 19: 2213.

[106] Zhang JH, Yang B. Adv. Funct. Mater. 2010; 20: 3411.

[107] He M, Wang JX, Li HL, Jin XL, Wang JJ, Liu BQ, Song YL. Soft Matter 2010; 6: 2396.

[108] He M, Wang JX, Li HL, Song YL. Soft Matter 2011; 7: 3993.

[109] Jung S, Dorrestijn M, Raps D, Das A, Megaridis CM, Poulikakos D. Langmuir 2011; 27: 3059.

[110] Meuler AJ, Smith JD, Varanasi KK, Mabry JM, McKinley GH, Cohen RE. ACS Appl. Mater. Interface 2010; 2: 3100.

[111] Balu B, Berry AD, Hess DW, Breedveld V. Lab Chip 2009; 9: 3066.

[112] Shi LT, Jiang CG, Ma MJ, Wu CW. Biomicrofluidics 2010; 4: 041101.

[113] Chunder A, Etcheverry K, Longde G, Cho HJ, Zhai L. Colloids Surf. A 2009; 333: 187.

[114] Bormashenko E, Pogreb R, Bormashenko Y, Musin A, Stein T. Langmuir 2008; 24: 12119.

[115] ZhaoY, Fang J, Wang HX, Wang XG, Lin T. Adv. Mater. 2010; 22: 707.

[116] Zheng YM, Bai H, Huang ZB, Tian XL, Nie FQ, Zhao Y, Zhai J, Jiang L. Nature 2010; 463: 640.

[117] Bai H, Tian XL, Zheng YM, Ju J, Zhao Y, Jiang L. Adv. Mater. 2010; 22: 5521.

[118] Shirtcliffe NJ, McHale G, Newton MI. Langmuir 2009; 25: 14121.

[119] Parker AR, Lawrence CR. Nature 2001; 414: 33.

[120] Zhai L, Berg MC, Cebeci FC, Kim Y, Milwid JM, Rubner MF, Cohen RE. Nano Lett. 2006; 6: 1213.

[121] Dorrer C, Ruhe J. Langmuir 2008; 24: 6154.

[122] Garrod RP, Harris LG, Schofield WCE, McGettrick J, Ward LJ, Teare DOH, Badyal JPS. Langmuir 2007; 23: 689.

[123] Lee CH, Johnson N, Drelich J, Yap YK. Carbon 2011; 49: 669.

[124] Li HL, Wang JX, Yang LM, Song YL. Adv. Funct. Mater. 2008; 18: 3258.

[125] Zhu Q, Tao F, Pan QM. ACS Appl. Mater. Interfaces 2010; 1: 3141.

[126] Feng L, Zhang ZY, Mai ZH, Ma YM, Liu BQ, Jiang L, Zhu DB. Angew. Chem. Int. Ed. 2004; 43: 2012.

[127] Ben W, Liang WX, Guo ZG, Liu WM. Chem. Soc. Rev. 2015; 44: 336.

[128] Yuan JK, Liu XG, Akbulut O, Hu JQ, Suib SL, Kong J, Stellacci F. Nat. Nanotechnol. 2008; 3: 332.

[129] Gui CX, Wei JW, Wang KL, Cao AY, Zhu HW, Jia Y, Shu Q, Wu DH. Adv. Mater. 2010; 22: 617.

[130] Koc K, de Mello AJ, McHale G, Newton MI, Roach P, Shirtcliffe NJ. Lab Chip 2008; 8: 582.

[131] Zhang XX, Wang L, Levanen E. RSC Adv. 2013; 3: 12003.

[132] Yang Y, Lai YK, Zhang QQ, Wu K, Zhang LH, Lin CJ, Tang PF. Colloids Surf. B 2010; 79: 309.

[133] Huang YX, Lai YK, Lin LX, Sun L, Lin CJ. Acta Phys.-Chim. Sin. 2010; 26: 2057.

[134] Ishizaki T, Saito N, Takai O. Langmuir 2010; 26: 8147.

[135] Chen L, Liu MJ, Bai H, Chen PP, Xia F, Han D, Jiang L. J. Am. Chem. Soc. 2009; 131: 10467.

[136] Genzer J, Efimenko K. Biofouling 2006; 22: 339.

[137] Zhou M, Yang JH, Ye X, Zheng AR, Li G, Yang, Zhu Y, Cai L. J. Nano Res. 2008; 2: 129.

[138] Mao C, Liang CX, Luo WP, Bao JC, Shen J, Hou XM, Zhao WB. J. Mater. Chem. 2009; 19: 9025.

[139] Hou XM, Wng XB, Zhu QS, Bao JC, Mao C, Jiang LC, Shen JA. Colloids Surf. B 2010; 80: 247.

[140] Lai YK, Sun L, Chen YC, Zhuang HF, Lin CJ, Chin JW. J. Electrochem. Soc. 2006; 153: D123.

[141] Zhuang HF, Lin CJ, Lai YK, Sun L, Li J. Environ. Sci. Technol. 2007; 41: 4735.

[142] Lai YK, Huang JY, Zhang HF, Subramaniam VP, Tang YX, Gong DG, Sundar L, Sun L, Chen Z, Lin CJ. J. Hazard. Mater. 2010; 184: 855.

[143] Soliveri G, Annunziata R, Ardizzone S, Cappelletti G, Meroni D. J. Phys. Chem. C 2012; 11: 26405.

[144] Pittrof A, Bauer S, Schmuki P. Acta Biomater. 2011; 7: 424.

[145] Lai YK, Lin CJ, Wang H, Huang JY, Zhuang HF, Sun L. Electrochem. Commun. 2008; 10: 387.

[146] Nakata K, Nishimoto S, Yuda Y, Ochiai T, Murakami T, Fujishima A. Langmuir 2010; 26: 11628.

[147] Nishimoto S, Sekine H, Zhang XT, Liu ZY, Nakata K, Murakami T, Koide Y, Fujishima A. Langmuir 2009; 25: 7226.

[148] Kinoshita H, Ogasahara A, Fukuda Y, Ohmae N. Carbon 2010; 48: 4403.

[149] Lai YK, Huang JY, Gong JJ, Huang YX, Wang CL, Chen Z, Lin CJ. J. Electrochem. Soc. 2009; 156: D480.

[150] Lai YK, Lin ZQ, Huang JY, Sun L, Chen Z, Lin CJ. New J. Chem. 2010; 34: 44.

[151] Lai YK, Lin ZQ, Chen Z, Huang JY, Lin CJ. Mater. Lett. 2010; 64: 1309.

[152] Huang YX, Sun L, Xie KP, Lai YK, Biu BJ, Ren B, Lin CJ. J. Raman Spectrosc. 2011; 42: 986.

[153] Lai YK, Huang YX, Wang H, Huang JY, Chen Z, Lin CJ. Colloids Surf. B 2010; 76: 117.

[154] Bekou S, Mattia D. Curr. Opin. Colloid Interface Sci. 2011; 16: 259.

[155] Watanabe, Yanuar, Udagawa H. J. Fluid Mech. 1999; 381: 225.

[156] Song Y, Nair RP, Zou M, Wang YA. Thin Solid Films 2010; 518: 3801.

[157] Cottin-Bizonne C, Barrat JL, Bocquet L, Charlaix E. Nat. Mater. 2003; 2: 237.

[158] Shirtcliffe NJ, MaHale G, Newton MI, Zhang Y. ACS Appl. Mater. Interface 2009; 1: 1316.

[159] Maboudian R, Howe RT. J. Vac. Sci. Technol. B 1997; 15: 1.

[160] Li L, Liu ZY, Zhang QQ, Meng CH, Zhang TR, Zhai J. J. Mater. Chem. A 2015; 3: 1279.

[161] Lai YK, Tang YX, Gong JJ, Gong DG, Chi LF, Lin CJ, Chen Z. J. Mater. Chem. 2012; 22: 7420.

[162] Wang F, Zhang G, Zhao Z, Tan H, Yu W, Zhang X, Sun Z. RSC Adv. 2015; 5: 9861.

[163] Kartini I, Santosa SJ, Febriyanti E, Nugroho OR, Yu H, Wang LZ. J. Nanoparticle Res. 2014; 16: 2514.

[164] Ding XF, Zhou SX, Gu GX, Wu LM. J. Mater. Chem. 2011; 21: 6161.

[165] Kamegawa T, Shimizu Y, Yamashita H. Adv. Mater. 2012; 24: 3697.

[166] Gao XF, Yan X, Yao X, Xu L, Zhang K, Zhang JH, Yang B, Jiang L. Adv. Mater. 2007; 19: 2213.

[167] Shen YZ, Tao HJ, Chen SL, Zhu LM, Wang T, Tao J. RSC Adv. 2015; 5: 1666.

[168] Hu YW, Huang SY, Liu S, Pan W. Appl. Surf. Sci. 2012; 258: 7460.

[169] Mahalakshmi PV, Vanithakumari SC, Gopal J, Mudali UK, Raj B. Curr Sci. 2011; 101: 1328.

[170] Shen GX, Chen YC, Lin L, Lin CJ, Scantlebury D. Electrochim. Acta 2015; 50: 5083.

[171] Shen GX, Chen YC, Lin CJ. Thin Solid Films 2005; 489: 130.

[172] Lai YK, Tang YX, Huang JY, Pan F, Chen Z, Zhang KQ, Fuchs H, Chi LF. Sci. Rep. 2013; 3: 3009.

[173] Huang JY, Li SH, Ge MZ, Wang LN, Xing TL, Chen GQ, Liu XF, Al-Deyab SS, Zhang KQ, Chen T, Lai YK. J. Mater. Chem. A 2015; 3: 2825.

[174] Wu SL, Weng ZY, Liu XM, Yeung KWK, Chu PK. Adv. Funct. Mater. 2014; 24: 5464.

[175] Li HQ, Lai YK, Huang JY, Tang YX, Yang L, Chen Z, Zhang KQ, Wang XC, Tan LP. J. Mater. Chem. B 2015; 3: 342.

[176] Huo KF, Gao B, Fu JJ, Zhao LZ, Chu PK. RSC Adv. 2014; 4: 17300.

[177] Tang PF, Zhang W, Wang Y, Zhang BX, Wang H, Lin CJ, Zhang LH. J. Nanomater. 2011; 2011: 178921.

[178] Amos FF, Morin SA, Streifer JA, Hamers RJ, Jin S. J. Am. Chem. Soc. 2007; 129: 14296.

[179] Segalman RA. Mater. Sci. Eng. R 2005; 48: 191.

[180] Liu SH, Wang WCM, Mannsfeld SCB, Locklin J, Erk P, Gomez M, Richter F, Bao ZN. Langmuir 2007; 23: 7428.

[181] Yoshimura M, Gallage R. J. Solid State Electrochem. 2008; 12: 775.

[182] Bessonov A, Kim JG, Seo JW, Lee JW, Lee S. Macromol. Chem. Phys. 2010; 211: 2636.

[183] Lai YK, Lin LX, Pan F, Huang JY, Song R, Huang YX, Lin CJ, Fuchs H, Chi LF. Small 2013; 9: 2945.

[184] Zhou, SX, Ding, XF, Wu, LM. Prog. Org. Coat. 2013; 76: 563.